Theoretically predicted effects of Gaussian curvature on lateral diffusion of membrane molecules

Tomoyoshi Yoshigaki*
HDA Biological Laboratory, 4-4-16-305 Izumi-chou, Nishi Tokyo, Tokyo 202-0011, Japan
(Received 12 September 2006; revised manuscript received 23 January 2007; published 2 April 2007)

Lateral diffusion on curved biological membranes has been studied theoretically and experimentally. However, how membrane geometries influence the diffusion process remains unclear. Here we show the significance of Gaussian curvature by numerically solving the diffusion equation in a geodesic polar coordinate system with regard to several types of surfaces including elliptic and hyperbolic paraboloids. On surfaces where Gaussian curvature has positive and negative values, diffusion is slower and faster than on the plane, respectively. The deviation from the normal diffusion on the plane tends to get larger as the absolute value of Gaussian curvature increases. Diffusion is anisotropic at a surface region where the normal curvature is anisotropic and Gaussian curvature has nonzero values. The anisotropy can be classified into several types according to whether diffusion is the fastest or the slowest in the principal directions. In the case of diffusion on spheroids, the limited area of a closed surface reduces the diffusion rate so greatly that the slowdown effects of positive values of Gaussian curvature are concealed. Analysis of the diffusion equation suggests that Gaussian curvature causes slowed or accelerated diffusion and anisotropic diffusion in any type of surface. Furthermore, it is discussed the degree to which Gaussian curvature influences diffusive phenomena taking place in real membranes through such effects. These results provide a different image of biological membranes that lateral diffusion of membrane molecules is usually anisotropic and the diffusion rate kaleidoscopically changes according to place.

DOI: 10.1103/PhysRevE.75.041901 PACS number(s): 87.15.Vv, 87.16.Dg, 87.16.Ac, 02.40.Ky

I. INTRODUCTION

The lateral diffusion of membrane proteins and lipids has been considered as important biological phenomena. One of the reasons is that many chemical reactions in biological membranes are caused by the collision among membrane molecules through lateral diffusion. So cellular events via membranes such as signal transduction, exo- and endocytosis, and reorganization of membrane cytoskeletons may be influenced by how membrane molecules laterally diffuse in the membranes. Fluorescence recovery after photobleaching (FRAP), single-particle tracking (SPT), and fluorescence correlation spectroscopy (FCS) are used as techniques to investigate the kinetic properties of membrane molecules, especially their diffusion rates. Analyses of the experimental data have revealed that, in some cases, diffusion proceeds at a different rate from the conventional diffusion on the plane. While the mean-square displacement is usually proportional to time, some proteins of the plasma membrane do not obey this rule [1–3]. Such anomalous diffusion is attributed mainly to interactions with obstacles such as cytoskeletal structures beneath membranes although other potential mechanisms have been studied [4]. On the other hand, Smith *et al.* [5] found that membrane glycoproteins on the surface of mouse fibroblasts diffuse faster in the direction parallel to stress fibers than in the direction perpendicular to them. It seems that the membrane proteins are prevented from crossing the fibers and consequently anisotropic diffusion takes place. Furthermore, de Monvel *et al.* [6] recently demonstrated orthotropic diffusion of membrane lipids in outer hair cells, suggesting that it is due to the orthotropic membrane skeleton.

In addition to interactions with cytoskeletal structures, membrane geometries are thought as one of possible factors that cause anomalous and anisotropic diffusions. If so, experimental data are extensively influenced by membrane geometries because most biological membranes take the shape of surfaces, but not the plane. Effects of membrane geometries on FRAP and FCS data have been studied through simulations of diffusion on various surfaces, for example, a wavy surface like membranes with many microvilli [7], a corrugated surface in one direction [8], periodic nodal surfaces [9], surfaces of elliptic and hyperbolic paraboloids [3], and surfaces computationally reconstructed from image data of real membranes of the endoplasmic reticulum [10]. These simulations indicate that the diffusion rate on surfaces frequently looks smaller than the real one. For a simple instance, on a corrugated surface only in the x direction, diffusion appears to be slower in the x direction than in the y direction if viewed from the z axis [8]. It looks as if anisotropic diffusion took place although this is an effect of projection. FCS data obtained through Monte Carlo simulations indicate that the mobility of membrane molecules on parabolic surfaces is remarkably underestimated [3]. However, it is reported in the paper that the fractal analyses of the simulated FCS data do not show any hint of anomalous diffusion. So membrane geometries of surfaces have "apparent" effects on FRAP and FCS data. If geometric effects are limited to the apparent effects, anomalous and anisotropic diffusions never take place on curved membranes in an "essential" sense. However, it remains to be examined whether membrane geometries have essential effects on the diffusion process.

The fundamental equation regarding diffusion on surfaces is the continuity equation in a two-dimensional manifold and

*FAX: +81 42-423-0180. Electronic address: sv5t-ysgk@asahi-net.or.jp

has been used in many studies [3,7,8]. By solving the equation in each case, we can simulate movements of membrane molecules even if the molecules flow in the field of conservative force [11,12]. However, it is difficult to find out essential effects of membrane geometries in such simulations because most coordinate systems used for describing the diffusion equations are not suitable to compare the diffusive behavior on surfaces with that on the plane. For instance, if a coordinate system of u and v is defined on a surface, the distance between a point of (u,v) and the origin of $(u=0, v=0)$ is not necessarily equal to $(u^2+v^2)^{0.5}$. The concept of geodesic lines is necessary for calculating the distance between the two surface points. In the present study, we simulate diffusion on various surfaces by defining a geodesic polar coordinate system of r and θ on them. The parameter r represents the distance from the origin in both cases of surfaces and the plane. This method makes it possible to directly compare the diffusion length on surfaces with that on the plane. So essential effects of membrane geometries, especially effects of Gaussian curvature, can be extracted from the simulations. Indeed, Christensen [13] previously pointed out the significance of using geodesic lines in simulations of diffusion on surfaces. The present simulations reveal that positive and negative values of Gaussian curvature make diffusion slower and faster than the normal diffusion on the plane, respectively. Moreover, anisotropy of the normal curvature causes anisotropic diffusion only in surface regions where Gaussian curvature has nonzero values. Such unusual diffusions take place in an essential, but not apparent, sense.

II. METHODS

A. Equation of diffusion on surfaces

The molecular concentration C on surfaces is a function of the position x^1 and x^2 and the time t. The continuity equation is expressed as

$$D^{-1}C_t = g^{ij}\nabla_i\nabla_j C \quad (i,j=1,2), \tag{1}$$

where D is a diffusion coefficient. C_t is the derivative with respect to t, and g^{ij} is the metric. ∇_i is the covariant derivative with respect to x^i. The summation rule of Einstein is used in the right-hand side. Any type of coordinate systems can be selected for x^1 and x^2 as long as points on a surface are associated with the coordinates by one-to-one correspondence. In the present simulations, a polar coordinate system is defined on surfaces and therefore r and θ are used as x^1 and x^2, respectively. While it is easy to define a polar coordinate system on the plane, the concept of geodesic lines is necessary for the definition on surfaces. A point on a surface is selected for the point of $r=0$. In the case of the plane, straight lines passing through the point of $r=0$ are used to assign polar coordinates (r,θ) to points. In the case of surfaces, geodesic lines passing through the point of $r=0$ are used instead. If a surface point is located on such a geodesic line, values of r and θ at the point indicate the length from the point of $r=0$ along the geodesic line and the angle between the geodesic line and the standard geodesic line of $\theta=0$. Values of r and θ vary on the intervals $-\infty \leqslant r \leqslant +\infty$ and $0 \leqslant \theta < \pi$. The Riemannian metric can be expressed as

$$ds^2 = dr^2 + G\,d\theta^2, \tag{2}$$

where G is a function of r and θ. Since it means $g_{11}=1$, $g_{12}=0$, and $g_{22}=G$, Eq. (1) is transformed into

$$D^{-1}C_t = C_{rr} + 0.5G^{-1}G_rC_r + G^{-1}C_{\theta\theta} - 0.5G^{-2}G_\theta C_\theta, \tag{3}$$

where lowered indexes r, θ, and t denote the first and second derivatives of C and G with respect to them. Since G is equal to r^2 in the case of the plane, Eq. (3) takes the form of

$$D^{-1}{}_pC_t = {}_pC_{rr} + r^{-1}{}_pC_r + r^{-2}{}_pC_{\theta\theta}, \tag{4}$$

where ${}_pC$ is used instead of C to stress the plane, but not surfaces.

B. Calculation of a function G

Calculation of G in each surface is essential for obtaining the diffusion equation (3). Since it is difficult to analytically calculate $G(r,\theta)$, the function is numerically calculated. If a surface is viewed as embedded in a three-dimensional space where a Cartesian coordinate system is defined, the position vector of a surface point can be expressed as $\boldsymbol{P}=(x,y,z)$. A two-dimensional coordinate system of u and v is defined on the surface. The coordinate system of u and v is properly selected according to types of surfaces and does not have to match the polar coordinate system of r and θ. The components x, y, and z of the vector $\boldsymbol{P}$ are regarded as functions of u and v, and the two parameters are regarded as functions of r and θ. First, we calculate the first and second derivatives of the vector $\boldsymbol{P}$ with respect to u and v, and therefore obtain two 3×3 matrices $(\boldsymbol{P}_u\boldsymbol{P}_v\boldsymbol{e}_n)$ and $(\boldsymbol{P}_{uu}\boldsymbol{P}_{uv}\boldsymbol{P}_{vv})$. Here all the vectors are column vectors and $\boldsymbol{e}_n$ denotes the normal unit vector. Christoffel's symbol Γ is calculated from the two matrices as

$$(\boldsymbol{P}_u\boldsymbol{P}_v e_n)^{-1}(\boldsymbol{P}_{uu}\boldsymbol{P}_{uv}\boldsymbol{P}_{vv}) = \begin{pmatrix} \Gamma^u_{uu} & \Gamma^u_{uv} & \Gamma^u_{vv} \\ \Gamma^v_{uu} & \Gamma^v_{uv} & \Gamma^v_{vv} \\ \Gamma_{uu} & \Gamma_{uv} & \Gamma_{vv} \end{pmatrix}. \tag{5}$$

This formula can be obtained from the definition of Christoffel's symbol Γ, i.e., $\boldsymbol{P}_{ij}=\boldsymbol{P}_\alpha\Gamma^\alpha_{ij}+\mathbf{e}_n\Gamma_{ij}$ [14]. The functions $u(r,\theta)$ and $v(r,\theta)$ obey the geodesic equations

$$u_{rr} = -\Gamma^u_{uu}u_r^2 - 2\Gamma^u_{uv}u_rv_r - \Gamma^u_{vv}v_r^2, \tag{6}$$

$$v_{rr} = -\Gamma^v_{uu}u_r^2 - 2\Gamma^v_{uv}u_rv_r - \Gamma^v_{vv}v_r^2. \tag{7}$$

The case is considered in which values of $u(r,\theta)$, $v(r,\theta)$, $u_r(r,\theta)$, and $v_r(r,\theta)$ are given at a certain value of r. Values of $u_{rr}(r,\theta)$ and $v_{rr}(r,\theta)$ are calculated from the values of $u_r(r,\theta)$ and $v_r(r,\theta)$ using Eqs. (6) and (7). Then values of $u(r+\Delta r,\theta)$, $v(r+\Delta r,\theta)$, $u_r(r+\Delta r,\theta)$, and $v_r(r+\Delta r,\theta)$ are numerically calculated from values of $u(r,\theta)$, $v(r,\theta)$, $u_r(r,\theta)$, $v_r(r,\theta)$, $u_{rr}(r,\theta)$, and $v_{rr}(r,\theta)$ through Euler's method. The functions $u(r,\theta)$, $v(r,\theta)$, $u_r(r,\theta)$, and $v_r(r,\theta)$ are thus calculated by starting from the values of $u(r=0)$, $v(r=0)$, $u_r(r=0,\theta)$, and $v_r(r=0,\theta)$. If the direction of $\boldsymbol{P}_u(r=0)$ is selected for the direction of the geodesic line of $\theta=0$,

$$u_r(r=0,\theta) = g_{11}^{-0.5}(\cos\theta - g^{-0.5}g_{12}\sin\theta), \tag{8}$$

$$v_r(r=0,\theta) = g^{-0.5}g_{11}^{0.5}\sin\theta, \tag{9}$$

where x^1 and x^2 represent u and v, respectively, and g denotes $g_{11}g_{22}-g_{12}^2$. These equations can be obtained from the relation $\boldsymbol{P}_r=\boldsymbol{P}_u u_r+\boldsymbol{P}_v v_r$. In the present simulations, the point of $u=0$ and $v=0$ is always selected for the point of $r=0$. Moreover, in all the cases, the coordinate system of u and v forms a two-dimensional Cartesian coordinate system locally in a small region around the point of $r=0$ because $\boldsymbol{P}_u$ and $\boldsymbol{P}_v$ are orthogonal unit vectors due to the way of selecting u and v, which is described below. This arrangement makes the calculation of the functions $u(r,\theta)$ and $v(r,\theta)$ easier because it provides $u(r=0)=0$, $v(r=0)=0$, $u_r(r=0,\theta)=\cos\theta$, and $v_r(r=0,\theta)=\sin\theta$. In actual simulations, $u(r,\theta)$ and $v(r,\theta)$ are calculated on the intervals $-2\leqslant r\leqslant 2$ μm and $0\leqslant\theta<\pi$ in steps of $\Delta r=2.0e-4$ μm and $\Delta\theta=0.01\pi$ rad. To prevent the point of $r=0$ from being one of the boundaries, r has both positive and negative values, that is, varies on the interval $(-\infty,\infty)$, by limiting θ to the interval $[0,\pi)$. The polar coordinate system is thus modified in terms of the range of r and θ. The functions $x(r,\theta)$, $y(r,\theta)$, and $z(r,\theta)$ are calculated from $u(r,\theta)$ and $v(r,\theta)$. Since G is equal to the inner product of $\boldsymbol{P}_\theta$, $G(r,\theta)$ is calculated using

$$G = x_\theta^2 + y_\theta^2 + z_\theta^2. \tag{10}$$

The diffusion equation (3) is determined by the function $G(r,\theta)$.

With regard to all surfaces treated in the present study, the components x and y of the vector $\boldsymbol{P}$ are used as u and v except for the case of spheroids. In other words, the vector $\boldsymbol{P}$ is expressed as $(x(x), y(y), z(x,y))$. In the case of spheroids, a two-dimensional Cartesian coordinate system is defined on the tangent plane touching the surface at the top point of a spheroid. A straight line connecting a point on the tangent plane and the bottom point of the spheroid passes through a point on the surface. Since one surface point is thus associated with one point on the tangent plane by one-to-one correspondence, we can use the Cartesian coordinates defined on the tangent plane as u and v.

Gaussian curvature K is expressed as

$$K = (\Gamma_{uu}\Gamma_{vv} - \Gamma_{uv}^2)g^{-1}. \tag{11}$$

The normal curvature λ at the point of $r=0$ is expressed as

$$\lambda = \Gamma_{uu}u_r^2 + 2\Gamma_{uv}u_r v_r + \Gamma_{vv}v_r^2. \tag{12}$$

Here the word "normal curvature" means the curvature of a curve in which a plane including the normal cuts the surface. If Eqs. (8) and (9) are substituted for Eq. (12), it takes the form of $A\sin(2\theta+B)+C$.

C. Solution of the diffusion equation

We investigated the diffusion that, at $t=0$, membrane molecules are confined in a circular region of radius ξ and the molecular concentration C within the region has a constant value C_0. The conditions are written as

$$C(|r|\leqslant\xi,\theta,t=0) = C_0, \tag{13}$$

$$C(|r|>\xi,\theta,t=0) = 0. \tag{14}$$

Taking these conditions as the initial conditions, Eq. (3) was numerically solved with regard to various surfaces. The way of solving the diffusion equation is described in the previous paper [11,12] although some modifications are performed in the following way. The numerical calculations of C_θ and $C_{\theta\theta}$ cause serious numerical instability probably because the difference between $C(r,\theta)$ and $C(r,\theta+\Delta\theta)$ is too small around the point of $r=0$. In numerical calculations, the difference between two values tends to have a larger error as they get closer to each other. Indeed, the numerical instability first appears around the point of $r=0$ and then spreads out toward the regions of larger values of r. To prevent the numerical instability, C_θ and $C_{\theta\theta}$ were assumed to be always zero in the case of $K>0$. The assumption is true only when a surface is symmetrical about the normal at the point of $r=0$. Other ways of calculations, at least ones we tried, caused numerical instability. In the case of $K<0$, C_θ was calculated in steps of $25\Delta r$, but not Δr, and a value of $\{C_\theta(r+25\Delta r,\theta) - C_\theta(r,\theta)\}(n/25)+C_\theta(r,\theta)$ was assigned to $C_\theta(r+n\Delta r,\theta)$, where n is an integer that varies from 1 to 24. $C_{\theta\theta}$ was similarly calculated. This way prevented the numerical instability. The values of Δr, $\Delta\theta$, and Δt are $2.0e-2$ μm, 0.01π rad, and $3.162e-6$ s in all the simulations, except for the simulation of diffusion on spheroids in which Δr is $5.0e-3$ μm (see the legend of Fig. 6). The solution $C(r,\theta)$ is calculated on the intervals $-2\leqslant r\leqslant 2$ μm and $0\leqslant\theta<\pi$. The boundary conditions are

$$C_r(r=\pm 2.0,\theta) = 2C_r(r=\pm 2.0 - \pm\Delta r,\theta) - C_r(r=\pm 2.0 - \pm 2\Delta r,\theta), \tag{15}$$

$$C_{rr}(r=\pm 2.0,\theta) = 2C_{rr}(r=\pm 2.0 - \pm\Delta r,\theta) - C_{rr}(r=\pm 2.0 - \pm 2\Delta r,\theta). \tag{16}$$

These formulas provide the way to estimate the values of C_r and C_{rr} at the point just on the boundary from the values at the two neighboring points. The value at the point nearest to the boundary is assumed to be equal to the average value between the point just on the boundary and the second nearest point. To calculate the graphs of this paper, 0.1 μm and $3.162e-9$ cm^2 s^{-1} were used as values of ξ and D. The value 3.162 is approximately equal to $1e+0.5$, that is, the square root of 10.

D. Calculations of $\langle r^2\rangle$ and $\langle r^2\rangle^*$

To examine how far membrane molecules move, $\langle r^2\rangle$ is defined in the following way. The sum of $r^2CG^{0.5}\,dr\,d\theta$ and the sum of $CG^{0.5}\,dr\,d\theta$ are calculated all over a surface from $C(r,\theta,t)$. Here the term $CG^{0.5}\,dr\,d\theta$ indicates an element of area. The ratio of the former to the latter is denoted by $\langle r^2\rangle$. In actual simulations, the sum of $r^2CG^{0.5}\Delta r\Delta\theta$ and the sum of $CG^{0.5}\Delta r\Delta\theta$ were calculated on the intervals $-2\leqslant r\leqslant 2$ μm and $0\leqslant\theta<\pi$, where Δr and $\Delta\theta$ are $2.0e-2$ μm and 0.01π rad. Although values of r are limited to such a

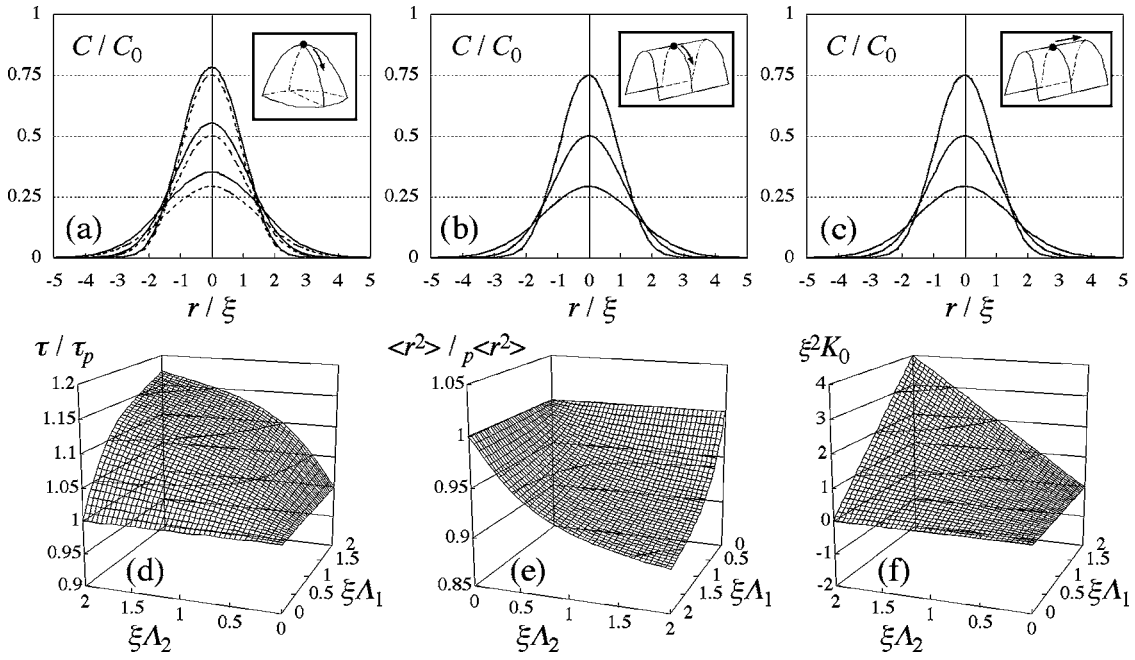

FIG. 1. Slowed diffusion on elliptic paraboloid. (a)–(c) Graphs of $C(r)$ at $t=0.5\tau_p$, τ_p, and $1.5\tau_p$ at a fixed value of θ with regard to diffusions on a surface (solid lines) and on the plane (dashed lines). Here τ_p is the time during which C at the zero point decreases to $0.5C_0$ on the plane. The ordinates and the abscissas represent C/C_0 and r/ξ. The values of $\xi\Lambda_1$, $\xi\Lambda_2$, and θ are (a) $\xi\Lambda_1=\xi\Lambda_2=2.0$, which represents a parabolic surface, and $\theta=0$, (b) $\xi\Lambda_1=2.0$, $\xi\Lambda_2=0$, which is a cylinder, and $\theta=0$, (c) the same cylinder and $\theta=0.5\pi$. Solid and dashed lines completely overlap in (b) and (c) so that the former conceals the latter. In each inset, the shape of the corresponding surface is illustrated. Small closed circle and arrow indicate the position of the zero point and the direction of the geodesic line along which each graph is calculated. (d)–(f) 3D graphs of τ/τ_p, $\langle r^2\rangle/{}_p\langle r^2\rangle$, and ξ^2K_0 that are functions of $\xi\Lambda_1$ and $\xi\Lambda_2$. Values of $\xi\Lambda_1$ and $\xi\Lambda_2$ are separately changed from 0 to 2.0 in steps of 0.05. To make a graph easy to see, the axes of $\xi\Lambda_1$ and $\xi\Lambda_2$ in (e) have the opposite direction to those in (d) and (f).

finite interval, the calculated sum is almost equal to the sum all over the surface because the finite interval corresponds to the interval $-20\leqslant r/\xi\leqslant 20$ and C is close to zero in the outside of the interval $-5\leqslant r/\xi\leqslant 5$ as shown in Fig. 1(a). Since all membrane molecules are not concentrated at the point of $r=0$ at $t=0$, $\langle r^2\rangle$ is not equivalent to the mean-square displacement in a strict sense. However, $\langle r^2\rangle$ provides some information about the diffusion length.

To examine how far membrane molecules move in the direction of each geodesic line, $\langle r^2\rangle^*$ is defined. The sum of $r^2CG^{0.5}\,dr$ and the sum of $CG^{0.5}\,dr$ are calculated all along a geodesic line of a fixed value of θ from $C(r,\theta,t)$. In actual simulations, the sum of $r^2CG^{0.5}\Delta r\Delta\theta$ and the sum of $CG^{0.5}\Delta r\Delta\theta$ were calculated on the interval $-2\leqslant r\leqslant 2$ μm at each value of θ. The ratio of the former to the latter is denoted by $\langle r^2\rangle^*$. While $\langle r^2\rangle$ is a function of t, $\langle r^2\rangle^*$ is one of θ and t. In the present simulations, the two functions are calculated at $t=\tau_p$, which represents the time during which C at the point of $r=0$ decreases to $0.5C_0$ in the case of diffusion on the plane (see Sec. III).

E. Programming

Programs are written in C++ and complied with C++ Builder 6 (Borland Software Corporation, Scotts Valley, CA). The graphs are made using Microsoft Excel (Microsoft, Redmond, WA).

III. RESULTS

Before performing simulations of diffusion on various surfaces, we provide a simple image of how the diffusion rate is affected by nonzero values of Gaussian curvature. A diffusing particle moves from one point to another point on a surface for a short time. On the surface, we can draw a small circle in such a manner that the starting point is the center of the circle and the terminal point is located within the circle almost certainly. The radius of the circle is determined by the diffusion coefficient and the observation time. In other words, if the two conditions remain unchanged, the circle has the same radius, on whichever surface diffusion takes place. Therefore the area of the circle is smaller and larger on surfaces of positive and negative values of K than on the plane, respectively. The probability that the particle exists within the circle just after the movement is almost equal to 1.0. The probability density is calculated by dividing the probability by the area. So the probability density is larger and smaller on surfaces of $K>0$ and $K<0$ than on the plane, respectively, if compared at points that are in the same distance from the center of the circle. Since the probability density has the same meaning as the molecular concentration, it is predicted that diffusion proceeds more slowly and faster on surfaces of $K>0$ and $K<0$ than on the plane, respectively. The image given here is discussed in more detail in Sec. IV B.

The comparison between the equations regarding diffusions on surfaces (3) and the plane (4) analytically supports

the prediction that the diffusion rate on surfaces of nonzero values of K deviates from the rate of the normal diffusion on the plane. In addition, the comparison indicates the possibility of anisotropic diffusion on surfaces where the geometry is anisotropic in the following way. The case is considered in which, at $t=t'$, $C(r,\theta)$ is a function of only r, i.e., $C_\theta=0$ and $C_{\theta\theta}=0$, and ${}_pC(r,\theta)$ is the same function as $C(r,\theta)$. In this case, Eqs. (3) and (4) are expressed as

$$D^{-1}C_t(r,\theta,t=t') = C_{rr} + 0.5G^{-1}G_rC_r, \tag{17}$$

$$D^{-1}{}_pC_t(r,\theta,t=t') = {}_pC_{rr} + r^{-1}{}_pC_r. \tag{18}$$

Since ${}_pC_{rr}$ and ${}_pC_r$ are equal to C_{rr} and C_r, the difference between the two equations gives

$$C_t(r,\theta,t=t') - {}_pC_t(r,\theta,t=t') = -Dr^{-1}C_rG^{-0.5}\int_0^r rG^{0.5}K\,dr. \tag{19}$$

The formula $K=-0.5G^{-1}G_{rr}+0.25G^{-2}G_r^2$ is used for the calculation of the right-hand side. If, at $r<0$ and $r\geqslant 0$, $C(r,t=t')$ is monotonically increasing and decreasing functions respectively, the term $-Dr^{-1}C_rG^{-0.5}$ is larger than zero at any value of r. Consequently, if K has positive values everywhere on a surface, the left-hand side of Eq. (19) is always positive, that is, C_t is larger than ${}_pC_t$ at every surface point. This is divided into several cases. If C_t has a negative value, ${}_pC_t$ has a negative value whose absolute value is larger than C_t. If C_t has a positive value, ${}_pC_t$ has a positive value whose absolute value is smaller than C_t or has a negative value. In all cases, the molecular concentration decreases more slowly or increases faster on the surface than on the plane. So, in the next time step, C gets a higher value at every surface point on the surface than on the plane, which means that diffusion is slowed down. In contrast, if K has negative values everywhere on a surface, C_t is smaller than ${}_pC_t$ at every surface point. The molecular concentration decreases faster or increases more slowly on the surface than on the plane. In the next time step, C gets a lower value at every surface point on the surface than on the plane, which means that diffusion is accelerated. If G is a function of not only r but also θ in Eq. (19), that is, if the geometry is anisotropic, the difference between C_t and ${}_pC_t$ varies according to θ as long as K has nonzero values. It means anisotropic diffusion. If K has negative values everywhere on a surface, diffusion is anisotropic because the geometry is anisotropic. On the other hand, if K has positive values everywhere on a surface, diffusion is not necessarily anisotropic. On some surfaces such as a parabolic surface, diffusion is isotropic because the geometry is isotropic and G is a function of only r. Note that, in the two cases of nonzero values of K, the difference between C_t and ${}_pC_t$ is a function of only r, but not equal to zero. If K is equal to zero everywhere on a surface, the difference between C_t and ${}_pC_t$ is zero at all surface points so that diffusion on the surface proceeds at the same rate as on the plane. In this case, diffusion is isotropic even if the geometry is anisotropic. Therefore Eq. (19) suggests that, on any types of surface, diffusion is slowed down and accelerated if K has positive and negative values, respectively. Furthermore, diffusion is anisotropic if K has nonzero values and the geometry is anisotropic. In the following sections, whether the prediction is true or not is examined through numerical solutions of Eq. (3).

A. Slowed diffusion on elliptic paraboloid

Diffusion on surfaces defined by

$$2Z = aX^2 + bY^2 \tag{20}$$

was examined. X, Y, and Z denote x/ξ, y/ξ, and z/ξ, respectively. ξ represents the radius of a circular region in which all membrane molecules are initially concentrated. The molecular concentration has a constant value C_0 inside the circular region and is equal to zero outside the region at $t=0$ [see Eqs. (13) and (14) in Sec. II C]. Dividing the length by ξ enables us to discuss the shape of surfaces without considering a length unit. The surface point of $x=0$ and $y=0$ is selected for the point of $r=0$. For the sake of convenience, the point of $r=0$ is called the zero point. The geodesic line that runs in the direction of the x axis at the zero point is selected for the line of $\theta=0$. The calculation using Eq. (12) indicates that the principal directions at the zero point correspond to the directions of the x axis and the y axis in the case of surfaces defined by Eq. (20). So $\theta=0$ and $\theta=0.5\pi$ represent the principal directions at the zero point. $C(r,\theta,t)$ is calculated by numerically solving Eq. (3) whose $G(r,\theta)$ is calculated using Eqs. (5)–(10) (see Sec. II).

Λ_1 and Λ_2 denote the principal curvatures at the zero point in the directions of the x axis and the y axis, respectively. Since a and b in Eq. (20) equal $\xi\Lambda_1$ and $\xi\Lambda_2$, respectively, the expressions $\xi\Lambda_1$ and $\xi\Lambda_2$ are used instead of a and b. One set of values of $\xi\Lambda_1$ and $\xi\Lambda_2$ represents an infinite number of surfaces because Λ_1 and Λ_2 have various values as a value of ξ is changed. However, such surfaces have the same shape because the change in a value of ξ is equivalent to only a change in a unit of the length. In other words, they are the same shape of surfaces with different sizes. One value of ξ determines one surface and further one diffusion because membrane molecules are initially confined in a circular region of radius ξ. While one set of values of $\xi\Lambda_1$ and $\xi\Lambda_2$ thus represents an infinite number of diffusions, they have the same properties as later elucidated in the Sec. IV A. We can obtain the information about all the diffusions by investigating one of them. In actual calculations, the diffusion in which ξ is 0.1 μm was simulated although any diffusion can be selected. In this and next sections, surfaces where both $\xi\Lambda_1$ and $\xi\Lambda_2$ have positive values are considered. They form elliptic paraboloid. Gaussian curvature K is expressed by

$$K = \Lambda_1\Lambda_2 g^{-2} \tag{21}$$

[see Eq. (11) in Sec. II]. This equation indicates that the sign of K at all surface points matches the sign of $\Lambda_1\Lambda_2$. So K has positive values everywhere on elliptic paraboloid. In Fig. 1(a), $\xi\Lambda_1$ and $\xi\Lambda_2$ have the same positive value. The molecular concentration C changed more slowly on the surface (solid lines) than on the plane (dashed lines). While a diffu-

sion along the geodesic line of $\theta=0$ is shown by the graph, the diffusions along all geodesic lines proceeded in the same way. It is because the surface is symmetrical about the z axis that corresponds to the normal at the zero point. If either $\xi\Lambda_1$ or $\xi\Lambda_2$ equals zero, surfaces form a cylinder where K is zero at every surface point as well as on the plane. Although the cylinder has no symmetry about the z axis, the diffusions along all geodesic lines proceeded at the same rate, irrespective of θ [Figs. 1(b) and 1(c)]. Moreover, the diffusion rate on the cylinder was identical to that on the plane. Since Eq. (1) is written using only the first fundamental quantities, it is natural that diffusion proceeds on the cylinder in the same way as on the plane. The graphs of Figs. 1(b) and 1(c) indicate that computer programs for solving Eq. (3) are created and work successfully. On the other hand, considering Fig. 1(a) together with Figs. 1(b) and 1(c), the diffusion rate may be influenced by Gaussian curvature.

To quantitatively analyze effects of Gaussian curvature on the diffusion rate, we calculated the time τ during which C at the zero point decreases to $0.5C_0$, i.e., $C(r=0,t=\tau)=0.5C_0$. When diffusion takes place on a surface represented by one set of values of $\xi\Lambda_1$ and $\xi\Lambda_2$, the ratio of τ to τ_p can be calculated. Here τ_p denotes τ with regard to diffusion on the plane in which ξ has the same value as diffusion on the surface. Figure 1(d) shows how the ratio τ/τ_p varies as values of $\xi\Lambda_1$ and $\xi\Lambda_2$ are changed separately. As $\xi\Lambda_1$ and $\xi\Lambda_2$ increased, the ratio τ/τ_p increased and so deviated from 1.0 more greatly. If either $\xi\Lambda_1$ or $\xi\Lambda_2$ was zero, the ratio τ/τ_p was always equal to 1.0. Concerning the diffusion length, the sum of $r^2CG^{0.5}\,dr\,d\theta$ and the sum of $CG^{0.5}\,dr\,d\theta$ are calculated all over a surface from the function of $C(r,\theta,t=\tau_p)$. The ratio of the former to the latter is denoted by $\langle r^2\rangle$ (see Sec. II). As $\xi\Lambda_1$ and $\xi\Lambda_2$ increased, the ratio of $\langle r^2\rangle$ to ${}_p\langle r^2\rangle$ decreased down from 1.0 [Fig. 1(e)]. Here ${}_p\langle r^2\rangle$ denotes $\langle r^2\rangle$ with regard to diffusion on the plane, which is defined in the same manner as τ_p. This result is consistent with Fig. 1(d). The two graphs indicate that diffusion is slower on surfaces of Eq. (20) than on the plane if K has positive values. The value of K at the zero point, which is denoted by K_0, equals the product of Λ_1 and Λ_2 [Fig. 1(f)]. Since the graphs of τ/τ_p and ξ^2K_0 are similar to each other [compare Fig. 1(d) with Fig. 1(f)], the degree to which diffusion is slowed down tends to get greater as K_0 increases. It remains to be examined whether the ratio τ/τ_p is a monotonically increasing function of K_0.

B. Anisotropic diffusion on elliptic paraboloid

If $\xi\Lambda_1$ and $\xi\Lambda_2$ have different positive values, diffusions along geodesic lines of $\theta=0$ and $\theta=0.5\pi$ proceeded in different ways [Figs. 2(a) and 2(b)]. To examine how fast diffusion along each geodesic line proceeds, we calculated the time ι during which C at $r=\xi$ decreases to $0.5C_0$, i.e., $C(r=\xi,\theta,t=\iota)=0.5C_0$. While ι is a function of θ in most cases, ι_p is constant, irrespective of θ. Here ι_p is ι with regard to diffusion on the plane. The ratio of ι to ι_p indicates the degree to which, along each geodesic line, diffusion on a surface deviates from the ordinary diffusion on the plane. By increasing $\xi\Lambda_2$ and keeping $\xi\Lambda_1$ constant, the shape of surfaces can be changed from a cylinder to a parabolic surface [illustrations on the right side of Fig. 2(c)]. The ratio ι/ι_p was the lowest at $\theta=0$ and the highest at $\theta=0.5\pi$ in all the shapes except that the ratio was constant in a cylinder and a parabolic surface [Fig. 2(c)]. To examine the diffusion length along each geodesic line, the sum of $r^2CG^{0.5}\,dr$ and the sum of $CG^{0.5}\,dr$ were calculated at a fixed value of θ from $C(r,\theta,t=\tau_p)$. The ratio of the former to the latter is denoted by $\langle r^2\rangle^*$ (see Sec. II). While $\langle r^2\rangle^*$ is a function of θ in most cases, ${}_p\langle r^2\rangle^*$ is constant, irrespective of θ. Here ${}_p\langle r^2\rangle^*$ is $\langle r^2\rangle^*$ with regard to diffusion on the plane. The ratio of $\langle r^2\rangle^*$ to ${}_p\langle r^2\rangle^*$ was the highest at $\theta=0$ and the lowest at $\theta=0.5\pi$ except for a cylinder and a parabolic surface [Fig. 2(d)]. This result is consistent with Fig. 2(c). The two graphs indicate that diffusion is anisotropic on most of the surfaces. The normal curvature at the zero point, which is denoted by λ, is a function of θ [Fig. 2(e) and see Eq. (12) in Sec. II]. The comparison between $\xi\lambda$ and $\langle r^2\rangle^*/{}_p\langle r^2\rangle^*$ indicates that diffusion is the fastest and the slowest in the directions of the maximum and minimum of λ, i.e., the principal directions, respectively [compare graph lines marked by small circles in Figs. 2(d) and 2(e)]. This kind of anisotropic diffusion is called the $+K1$ type [Fig. 2(f)]. If K_0 has a positive value, diffusion belongs to the $+K1$ type in most cases [white region in Fig. 2(g)]. If $\xi\Lambda_1$ and $\xi\Lambda_2$ have the same value or if either of them equals zero, diffusion is isotropic (black region). $\Delta\iota$ denotes the difference between the maximum and minimum values of ι. To estimate the degree of anisotropy, the ratio of $\Delta\iota$ to ι_p is calculated in diffusion on each surface determined by $\xi\Lambda_1$ and $\xi\Lambda_2$ [Fig. 2(h)]. The ratio $\Delta\iota/\iota_p$ increased as $\xi\Lambda_1$ and $\xi\Lambda_2$ increased at a fixed ratio of Λ_1 to Λ_2. The ratio $\Delta\iota/\iota_p$ is the largest in the case that the ratio of Λ_1 to Λ_2 is approximately 0.4/1 and 1/0.4 [ridges of the three-dimensional (3D) graph].

C. Diffusion on hyperbolic paraboloid

Diffusion on surfaces of Eq. (20) where $\xi\Lambda_1$ and $\xi\Lambda_2$ have positive and negative values, respectively, is considered in this section. They form a hyperbolic paraboloid and K has negative values everywhere as shown in Eq. (21). In Fig. 3(a), $\xi\Lambda_1$ and $\xi\Lambda_2$ have the same absolute value. In contrast to the case of positive values of K, diffusion proceeded faster on the surface (solid lines) than on the plane (dashed lines). As the absolute values of $\xi\Lambda_1$ and $\xi\Lambda_2$ increased, the ratio τ/τ_p decreased down from 1.0 [Fig. 3(b)] and the ratio $\langle r^2\rangle/{}_p\langle r^2\rangle$ increased up from 1.0 [Fig. 3(c)]. The two graphs indicate that diffusion is accelerated on surfaces of negative values of K. Furthermore, as the absolute value of K_0 increases, the diffusion rate tends to deviate from the rate of the normal diffusion on the plane more greatly. By increasing the absolute value of $\xi\Lambda_2$ and keeping $\xi\Lambda_1$ constant, the saddlelike shape can be made steeper [illustrations on the right side of Fig. 3(d)]. The comparison between $\langle r^2\rangle^*/{}_p\langle r^2\rangle^*$ [Fig. 3(d)] and $\xi\lambda$ [Fig. 3(e)] reveals two types of anisotropic diffusion. One type is that diffusion is the slowest in the direction of the maximum of λ and the fastest in the direction of the minimum [compare graph lines marked by small circles in Figs. 3(d) and 3(e)]. Since we can reverse the di-

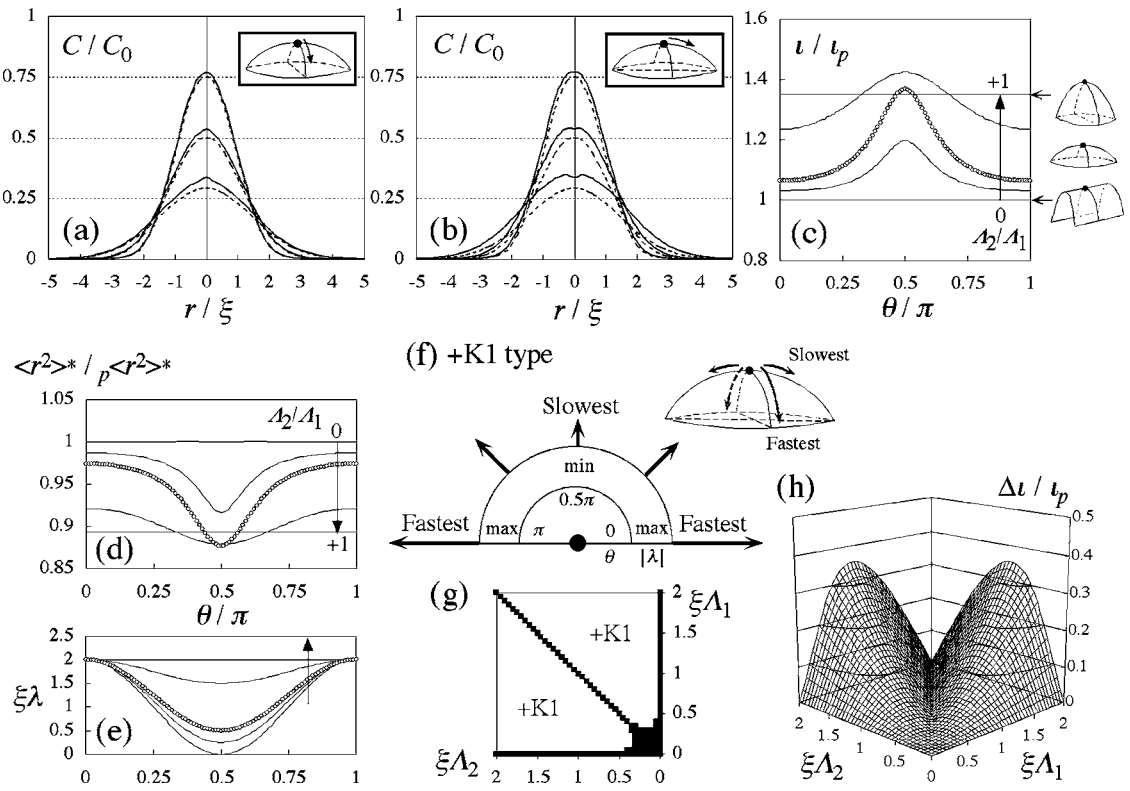

FIG. 2. Anisotropic diffusion on elliptic paraboloid. (a), (b) Graphs of $C(r)$ at $t=0.5\tau_p$, τ_p, and $1.5\tau_p$ at a fixed value of θ with regard to diffusions on the surface of $\xi\Lambda_1=2.0$ and $\xi\Lambda_2=0.8$ (solid lines) and on the plane (dashed lines). The value of θ is (a) $\theta=0$ and (b) $\theta=0.5\pi$. The graphs and insets are drawn in the same way as those of Fig. 1(a). (c)–(e) Graphs of ι/ι_p, $\langle r^2\rangle^*/{}_p\langle r^2\rangle^*$ and $\xi\lambda$ that are functions of θ. Graph lines represent diffusions on the surfaces where, at $\xi\Lambda_1=2.0$, $\xi\Lambda_2$ takes a value of 0, 0.25, 0.5 (line of small circles), 1.5, and 2.0 in the arrow direction. The shapes of the corresponding surfaces are illustrated on the right side of (c). The abscissas represent θ/π. (f) Diagram and the above-right illustration explain a type of anisotropic diffusion on elliptic paraboloid. A longer arrow represents a faster diffusion in its direction. For simplification, the direction of the maximum absolute value of λ is selected for $\theta=0$ in the diagram. This selection is peculiar to the diagrams of the figures. In solving Eq. (3), one of the principal directions is selected for $\theta=0$, whether λ has the maximum or the minimum in its direction (see the first paragraph in Sec. III A). So the direction of $\theta=0$ in the diagram does not necessarily match the direction of $\theta=0$ used throughout the present simulations. (g) The distribution of points of the coordinates $(\xi\Lambda_1, \xi\Lambda_2)$ representing surfaces where anisotropic (white region) and isotropic (black region) diffusions take place. (h) 3D graph of $\Delta\iota/\iota_p$ that is a function of $\xi\Lambda_1$ and $\xi\Lambda_2$. Values of $\xi\Lambda_1$ and $\xi\Lambda_2$ are separately changed from 0 to 2.0 in steps of 0.05 in (g) and (h).

rection of the axis of $\xi\lambda$ without changing the meaning of Fig. 3(e), a better expression is that diffusion is the slowest in one principal direction of the maximum absolute value of λ and the fastest in the other principal direction. This is called the $nK1$ type [Fig. 3(f)]. The other type is that diffusion is locally fastest in one principal direction of the maximum absolute value of λ, the slowest between two principal directions and the fastest in the other principal direction [compare thick lines in Figs. 3(d) and 3(e)]. This is called the $nK2$ type [Fig. 3(g)]. If the absolute values of $\xi\Lambda_1$ and $\xi\Lambda_2$ are so different, diffusion belongs to the $nK1$ type [white region in Fig. 3(h)]. If the two values are close to each other and large enough, diffusion belongs to the $nK2$ type (dotted region). The degree of anisotropy represented by the ratio $\Delta\iota/\iota_p$ increased as the absolute values of $\xi\Lambda_1$ and $\xi\Lambda_2$ increased at a fixed ratio of Λ_1 to Λ_2 [Fig. 3(i)]. The ratio $\Delta\iota/\iota_p$ is not equal to zero when the absolute values of $\xi\Lambda_1$ and $\xi\Lambda_2$ are identical to each other. It means that diffusion is anisotropic even if the principal curvatures Λ_1 and Λ_2 have the same absolute value, which is also shown in Fig. 3(h). The ratio $\Delta\iota/\iota_p$ is the largest in the case that the absolute value of Λ_1/Λ_2 is approximately 0.3/1 and 1/0.3 (ridges of the 3D graph).

D. Diffusion on catenoid

The simulations of diffusion on elliptic and hyperbolic paraboloids demonstrated that nonzero values of K make diffusion slower or faster than the normal diffusion on the plane and furthermore cause several types of anisotropic diffusion. Such phenomena, however, might be peculiar to the paraboloids. So diffusion on surfaces defined by

$$Z = a\cosh X + b\cosh Y, \tag{22}$$

was examined. The zero point of $r=0$ is placed at the surface point of $x=0$ and $y=0$. a and b in Eq. (22) equal $\xi\Lambda_1$ and $\xi\Lambda_2$, respectively. If both $\xi\Lambda_1$ and $\xi\Lambda_2$ have positive values, K is positive everywhere because of

$$K = \Lambda_1\Lambda_2 g^{-2}\cosh X\cosh Y. \tag{23}$$

In the case of diffusion on such surfaces, the ratio τ/τ_p was larger than 1.0 [Fig. 4(a)]. As a value of K_0 increases, the

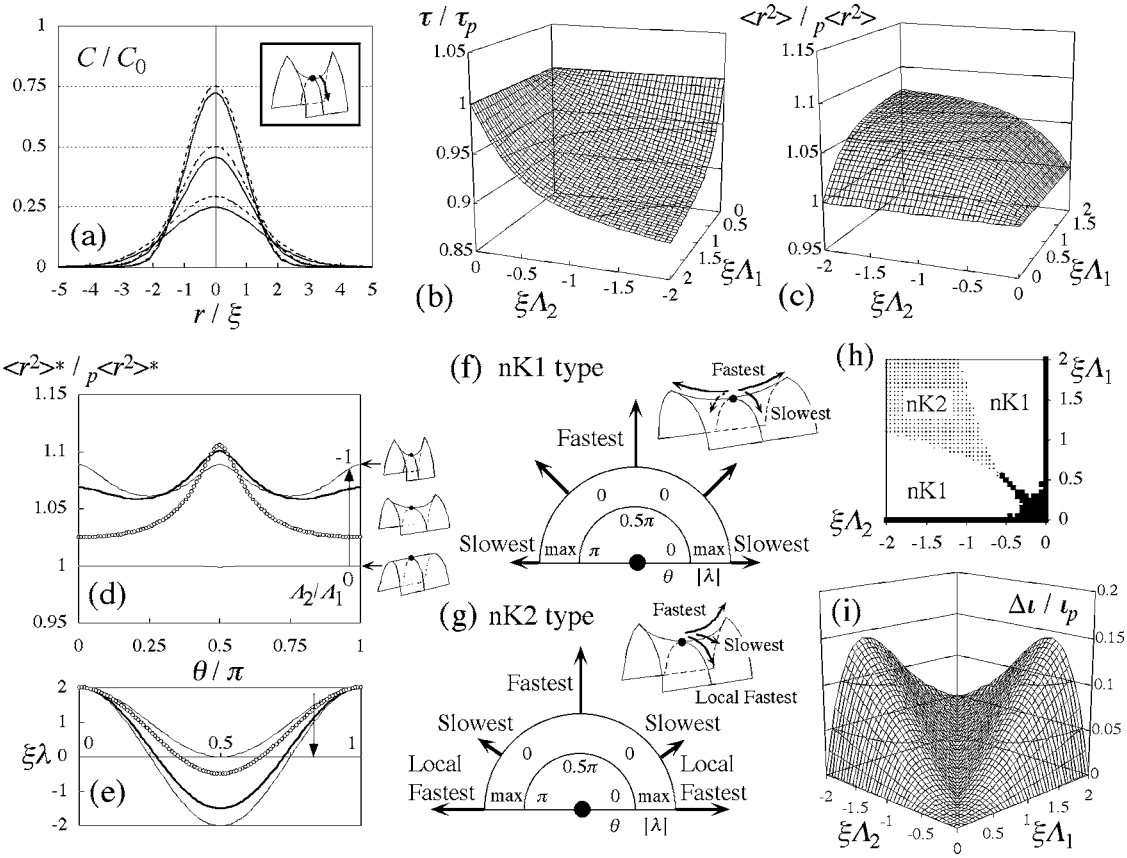

FIG. 3. Accelerated and anisotropic diffusion on hyperbolic paraboloid. (a) Graph of $C(r)$ at $t=0.5\tau_p$, τ_p, and $1.5\tau_p$, at $\theta=0$ with regard to diffusions on the surface of $\xi\Lambda_1=2.0$ and $\xi\Lambda_2=-2.0$ (solid lines) and on the plane (dashed lines). The graph and inset are drawn in the same way as those of Fig. 1(a). (b), (c) 3D graphs of τ/τ_p and $\langle r^2\rangle/{}_p\langle r^2\rangle$ that are functions of $\xi\Lambda_1$ and $\xi\Lambda_2$. The absolute values of $\xi\Lambda_1$ and $\xi\Lambda_2$ are separately changed from 0 to 2.0 in steps of 0.05 keeping $\xi\Lambda_1$ positive and $\xi\Lambda_2$ negative. Note the axes of $\xi\Lambda_1$ and $\xi\Lambda_2$ in (c) have the opposite direction to those in (b). (d), (e) Graphs of $\langle r^2\rangle^*/{}_p\langle r^2\rangle^*$ and $\xi\lambda$ that are functions of θ. Graph lines represent diffusions on the surfaces where, at $\xi\Lambda_1=2.0$, $\xi\Lambda_2$ takes a value of 0, −0.5 (lines of small circles), −1.5 (thick lines), and −2.0 in the arrow direction. The shapes of the corresponding surfaces are illustrated on the right side of (d). (f), (g) Diagrams and the above-right illustrations explain two types of anisotropic diffusion on hyperbolic paraboloid. They are drawn in the same way as those of Fig. 2(f). (h) The distribution of points of the coordinates $(\xi\Lambda_1, \xi\Lambda_2)$ representing surfaces where anisotropic (white and dotted regions) and isotropic (black region) diffusions take place. (i) 3D graph of $\Delta\iota/\iota_p$ that is a function of $\xi\Lambda_1$ and $\xi\Lambda_2$. Note that the ratio $\Delta\iota/\iota_p$ has nonzero values even if $\xi\Lambda_1$ and $\xi\Lambda_2$ have the same absolute value. Values of $\xi\Lambda_1$ and $\xi\Lambda_2$ in (h) and (i) are separately changed as in (b).

diffusion rate on the catenoid tends to more greatly deviate from that on the plane. In addition to the $+K1$ type, another type of anisotropic diffusion was found. The type is that diffusion is the fastest in one principal direction of the maximum of λ, the slowest between two principal directions and locally fastest in the other principal direction. This is called the $+K2$ type [Fig. 4(b)]. If values of $\xi\Lambda_1$ and $\xi\Lambda_2$ are close to each other, diffusion belongs to the $+K2$ type [Fig. 4(c)]. The degree of anisotropy represented by the ratio $\Delta\iota/\iota_p$ increased as values of $\xi\Lambda_1$ and $\xi\Lambda_2$ increased at a fixed ratio of Λ_1 to Λ_2 [Fig. 4(d)]. The ratio $\Delta\tau/\tau_p$ is the largest in the case that the ratio Λ_1/Λ_2 is approximately 0.4/1 and 1/0.4 (ridges of the 3D graph). While the graph patterns of Figs. 4(d) and 2(h) are similar to each other, the ratio $\Delta\iota/\iota_p$ is not completely equal to zero at $\xi\Lambda_1=\xi\Lambda_2$ in Fig. 4(d) unlike Fig. 2(h). In other words, diffusion is anisotropic to a small extent at $\xi\Lambda_1=\xi\Lambda_2$, which is also shown in Fig. 4(c). It is because the surfaces of Eq. (22) are not completely symmetrical about the z axis even though $\xi\Lambda_1$ and $\xi\Lambda_2$ have the same positive value.

If $\xi\Lambda_1$ and $\xi\Lambda_2$ have positive and negative values, respectively, K is negative everywhere as shown in Eq. (23). The ratio τ/τ_p was smaller than 1.0 [Fig. 4(e)]. As the absolute value of K_0 increases, the diffusion rate tends to more greatly deviate from that on the plane. In addition to the $nK1$ and $nK2$ types, another type of anisotropy was found. The type is that diffusion is the slowest in one principal direction of the maximum absolute value of λ, the fastest between two principal directions, and locally slowest in the other principal direction. This is called the $nK3$ type [Fig. 4(f)]. If the absolute values of $\xi\Lambda_1$ and $\xi\Lambda_2$ are close and small, the $nK3$ type of diffusion takes place [Fig. 4(g)]. The degree of anisotropy increased as $\xi\Lambda_1$ and $\xi\Lambda_2$ increased at a fixed ratio of Λ_1 to Λ_2 [Fig. 4(h)]. The ratio $\Delta\iota/\iota_p$ is the largest in the case that the ratio Λ_1/Λ_2 is approximately 0.3/1 and 1/0.3 (ridges of the 3D graph). Diffusion is not isotropic even though $\xi\Lambda_1$ and $\xi\Lambda_2$ have the same absolute value, which is also shown in Fig. 4(g). The graph pattern of Fig. 4(h) is similar to that of Fig. 3(i).

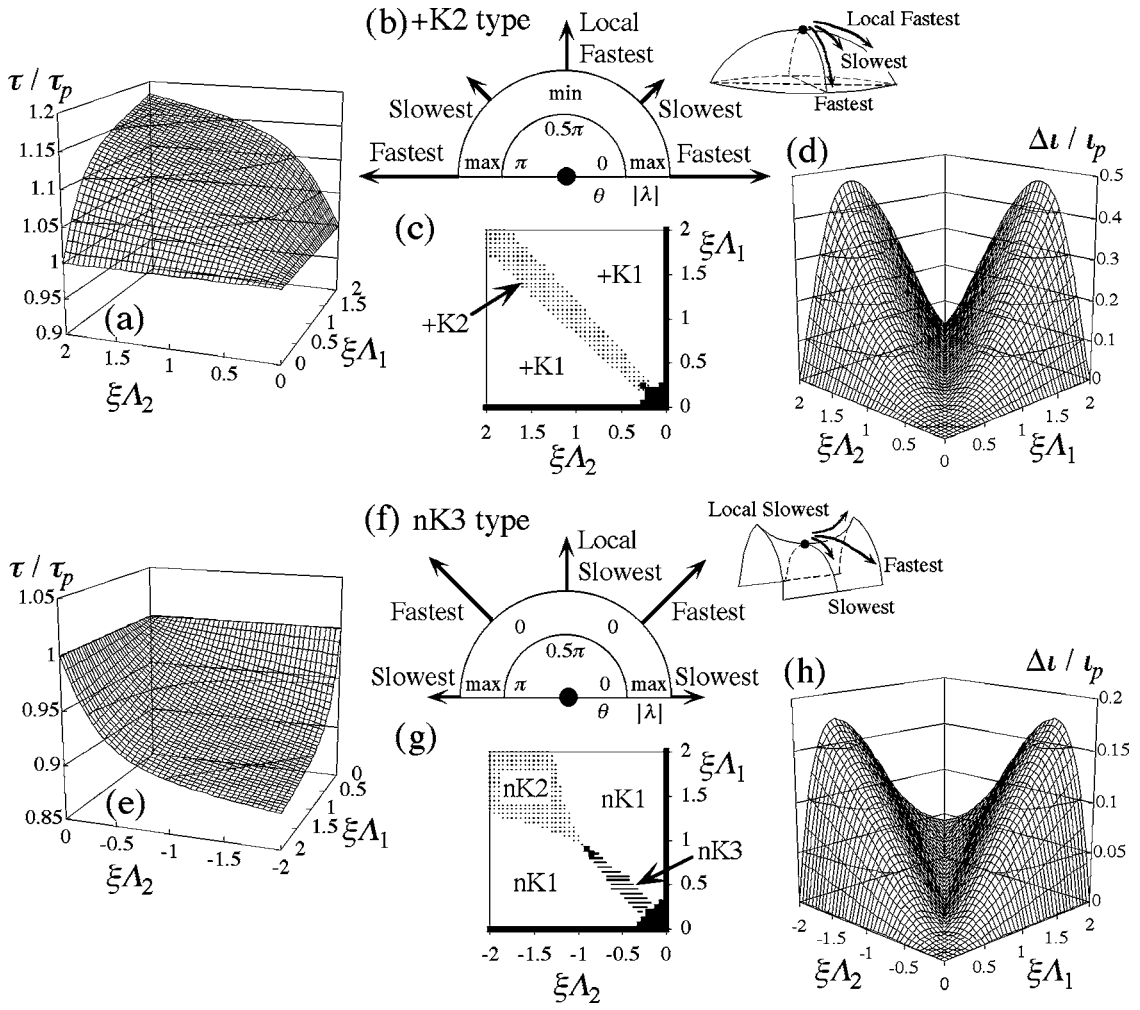

FIG. 4. Diffusion on catenoid. The cases of $K>0$ in (a)–(d) and $K<0$ in (e)–(h). (a) 3D graph of τ/τ_p that is a function of $\xi\Lambda_1$ and $\xi\Lambda_2$. Values of $\xi\Lambda_1$ and $\xi\Lambda_2$ are separately changed from 0 to 2.0 in steps of 0.05. (b) Diagram and the above-right illustration explain another type of anisotropic diffusion besides the $+K1$ type. (c) The distribution of points of the coordinates ($\xi\Lambda_1$, $\xi\Lambda_2$) representing surfaces where anisotropic (white and dotted regions) and isotropic (black region) diffusions take place. (d) 3D graph of $\Delta\iota/\iota_p$ that is a function of $\xi\Lambda_1$ and $\xi\Lambda_2$. Values of $\xi\Lambda_1$ and $\xi\Lambda_2$ are separately changed as in (a). (e) 3D graph of τ/τ_p that is a function of $\xi\Lambda_1$ and $\xi\Lambda_2$. The absolute values of $\xi\Lambda_1$ and $\xi\Lambda_2$ are separately changed from 0 to 2.0 in steps of 0.05 keeping $\xi\Lambda_1$ positive and $\xi\Lambda_2$ negative. (f) Diagram and the above-right illustration explain another type of anisotropic diffusion besides $nK1$ and $nK2$ types. (g) The distribution of points of the coordinates ($\xi\Lambda_1$, $\xi\Lambda_2$) representing surfaces where anisotropic (white, dotted, and striped regions) and isotropic (black region) diffusions take place. (h) 3D graph of $\Delta\iota/\iota_p$ that is a function of $\xi\Lambda_1$ and $\xi\Lambda_2$. Values of $\xi\Lambda_1$ and $\xi\Lambda_2$ are separately changed as in (e) although the axes of $\xi\Lambda_1$ and $\xi\Lambda_2$ have the opposite direction to those in the graph of τ/τ_p.

E. Slowed and accelerated diffusions on other surfaces

To examine whether slowed and accelerated diffusions take place on surfaces other than the paraboloids and the catenoids, diffusion on surfaces defined by the following equations was simulated:

$$Z = \cosh(aX^2 + bY^2)^{0.5}, \tag{24}$$

$$Z = a(X^2+1)^{0.5} + b(Y^2+1)^{0.5}, \tag{25}$$

$$Z = (aX^2 + bY^2 + 1)^{0.5}. \tag{26}$$

Here both a and b are limited to positive and zero values in Eqs. (24) and (26). Equation (24) represents a catenoid and Eqs. (25) and (26) represent hyperboloids. The zero point of $r=0$ is always placed at the surface point of $x=0$ and $y=0$ and therefore a and b of Eqs. (24)–(26) are equal to $\xi\Lambda_1$ and $\xi\Lambda_2$, respectively. Moreover, the sign of K at all surface points matches the sign of $K_0=\Lambda_1\Lambda_2$ because K is expressed in turn as

$$K = \Lambda_1\Lambda_2 g^{-2}(aX^2+bY^2)^{-0.5} \times \sinh(aX^2+bY^2)^{0.5}\cosh(aX^2+bY^2)^{0.5}, \tag{27}$$

$$K = \Lambda_1\Lambda_2 g^{-2}(X^2+1)^{-1.5}(Y^2+1)^{-1.5}, \tag{28}$$

$$K = \Lambda_1\Lambda_2 g^{-2}(aX^2+bY^2+1)^{-2}. \tag{29}$$

Figure 5 shows how the ratio τ/τ_p varies as values of $\xi\Lambda_1$ and $\xi\Lambda_2$ are changed keeping the two absolute values equal

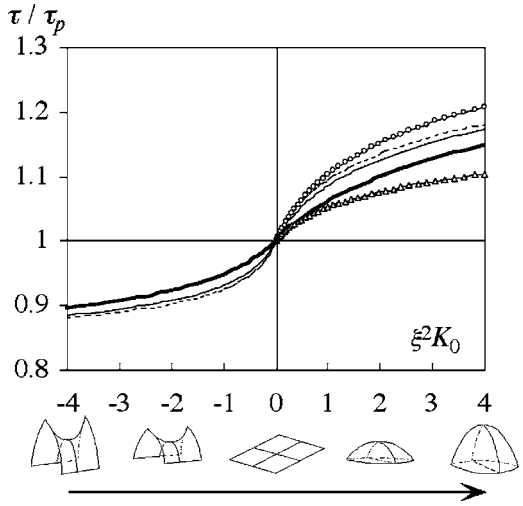

FIG. 5. Slowed and accelerated diffusions on various types of surfaces. A graph line represents a function τ/τ_p of ξ^2K_0 with regard to each surface. When a value of $\xi\Lambda_2$ is changed from −2.0 to 0 in steps of 0.05, a value of $\xi\Lambda_1$ is simultaneously changed from 2.0 to 0 keeping the value of $\xi\Lambda_1$ equal to the absolute value of $\xi\Lambda_2$. A value of ξ^2K_0 varied from −4.0 to 0. This is the negative side of the axis of abscissas. When a value of $\xi\Lambda_2$ is changed from 0 to 2.0 in steps of 0.05, a value of $\xi\Lambda_1$ is simultaneously changed from 0 to 2.0 keeping the value of $\xi\Lambda_1$ equal to the value of $\xi\Lambda_2$. A value of ξ^2K_0 varied from 0 to 4.0. This is the positive side of the axis of abscissas. Graph lines are shown on both positive and negative sides of the axis of abscissas in the cases of the paraboloid defined by Eq. (20) (thin solid line), the catenoid by Eq. (22) (dashed line), and the hyperboloid by Eq. (25) (thick solid line). On the other hand, graph lines are shown only on the positive side in the cases of the catenoid defined by Eq. (24) (line marked by small circles) and the hyperboloid by Eq. (26) (line marked by small triangles). Horizontal and vertical straight lines are drawn at the level of $\tau/\tau_p=1.0$ and at $\xi^2K_0=0$, respectively. The illustration below the graph shows how the shape of a surface changes. Arrow indicates the direction where ξ^2K_0 increases from a negative value to a positive value. As a value of ξ^2K_0 starts from −4.0 and approaches 0, the shape changes from a sharply curved saddle to a gently curved one. At $\xi^2K_0=0$, the plane appears. As a value of ξ^2K_0 starts from 0 and approaches 4.0, the shape changes from the tip of a blunt pen to a sharply pointed one. In any types of surface, the shape changes in a similar way.

to each other and keeping $\xi\Lambda_1$ positive. In the case of surfaces of Eq. (25), a value of $\xi\Lambda_2$ was changed from −2.0 to 2.0 so that the value of ξ^2K_0 varied from −4.0 to 4.0, that is, on both of positive and negative sides (thick solid line in Fig. 5). In the cases of surfaces of Eqs. (24) and (26), $\xi\Lambda_2$ was changed from 0 to 2.0 so that the value of ξ^2K_0 varied from 0 to 4.0, that is, only on the positive side (lines marked by small circles and triangles). The shape of surfaces changes as ξ^2K_0 varies (illustration below the graph). In any type of surfaces, the ratio τ/τ_p was larger and smaller than 1.0 if ξ^2K_0 had positive and negative values, respectively (Fig. 5). Furthermore, the ratio τ/τ_p deviated from 1.0 more greatly as the absolute value of ξ^2K_0 increased. These results indicate that the slowed diffusion in $K>0$ and the accelerated one in $K<0$ take place on various surfaces.

F. Slowed diffusion caused by the limited surface area

If K has positive values everywhere on a surface, the area is finite in some cases although the surfaces thus far simulated are not the case. The finite area may slow down diffusion if it is small. For instance, C at the zero point never decreases down to $0.5C_0$ on surfaces where the region of C_0 at $t=0$ covers more than half of the whole area. To examine how the limited area influences the diffusion process together with positive values of K, diffusion on the following surfaces was simulated:

$$a^{-2}X^2 + a^{-2}Y^2 + c^{-2}Z^2 = 1, \tag{30}$$

where values of a and c are positive. The surface forms a spheroid, which is a figure generated by rotating an ellipse about the z axis. The zero point of $r=0$ is placed at the surface point of $x=0$, $y=0$, and $z=c$. Since a is equal to $c^{0.5}(\xi^2K_0)^{-0.25}$, the shape is determined by values of ξ^2K_0 and c. In the other simulations, $\xi\Lambda_1$ and $\xi\Lambda_2$ are used as variables to determine the shape of a surface. In the case of spheroids, ξ^2K_0 is used instead because $\xi\Lambda_1$ and $\xi\Lambda_2$ always have the same positive value. The xy plane cuts the spheroid in a circle with radius of ξa, which equals $\xi c^{0.5}(\xi^2K_0)^{-0.25}$, and the z axis intersects it at $\pm\xi c$. As ξ^2K_0 increases at a fixed value of c, the spheroid takes a narrower shape, that is, becomes more prolate, and so the surface area decreases [Fig. 6(a)]. In contrast, as ξ^2K_0 decreases, the spheroid becomes more oblate and, at $\xi^2K_0=0$, the plane appears (dashed line). In the case of $c=0.5$, the ratio τ/τ_p rapidly increased as ξ^2K_0 increased and became extremely large around $\xi^2K_0\cong0.65$ [solid graph line of $c=0.5$ in Fig. 6(b)]. A quarter of the perimeter of the elliptical section by the zx plane is equal to ξ at $\xi^2K_0=0.72$. In other words, the area of the surface region of C_0 at $t=0$ is equal to half of the whole area. On the surface of $c=0.5$ and $\xi^2K_0=0.72$, C at the zero point decreases to be $0.5C_0$ for an infinite time and τ has an infinitely large value. Therefore the rapid slowdown of diffusion seems to be due to the limited area. As a value of c increased, the gradient of a graph line of τ/τ_p became smaller [see solid graph lines from the left to the right in Fig. 6(b)]. It means that, as a value of ξc increases at a constant value of ξ^2K_0, the ratio τ/τ_p decreases and the surface area increases. Therefore there is a strong possibility that an increase in the area reduces the degree to which diffusion is slowed down. Finally, the graph line of τ/τ_p approached the graph of diffusion on elliptic paraboloid [dashed graph line in Fig. 6(b)]. If c equals 2.0, a quarter of the perimeter of the elliptical section by the zx plane is equal to 2.4ξ even at $\xi^2K_0=4.0$. Since the perimeter is much larger than ξ, the finite area is unlikely to affect the diffusion process. The result of Fig. 6(b) indicates that, if the surface area is so small, it greatly slows down diffusion to conceal the effects of positive values of K. In addition, as the area increases, the effects of the finite area abruptly shrink and the slowdown of diffusion gets to be attributed only to positive values of K.

Simulations of diffusion on a sphere and a pseudosphere are a good idea for quantitatively analyzing the relationship between a change in the diffusion rate and a value of Gaussian curvature because K has constant positive and negative

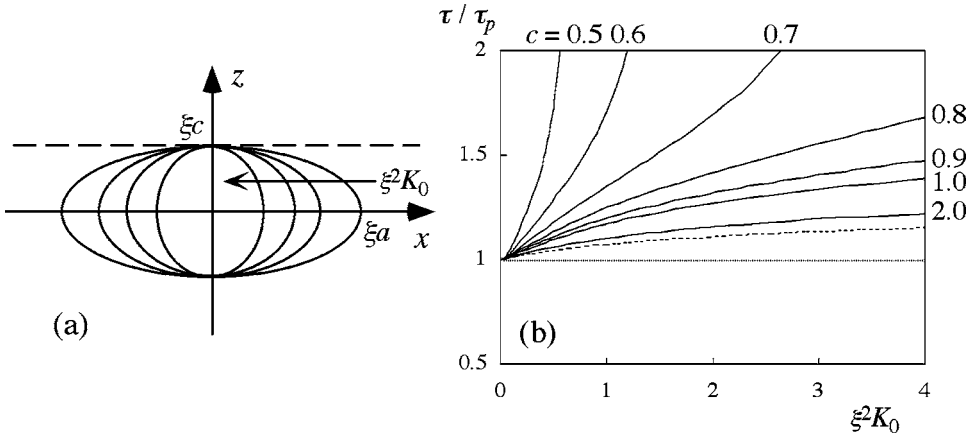

FIG. 6. Slowed diffusion on spheroids. (a) Elliptical sections of spheroids by the zx plane. The spheroids are symmetrical about the z axis. The shape of the sections changes in the arrow direction as a value of ξ^2K_0 increases at a fixed value of ξc. Conversely, as a value of ξ^2K_0 decreases and gets closer to zero, the shape approaches the plane represented by dashed line. (b) Graphs of functions τ/τ_p of ξ^2K_0 in each of which a value of ξc is fixed. A number beside each graph line indicates the corresponding value of c. Dashed line represents the function τ/τ_p of ξ^2K_0 in the case of parabolic surfaces, that is, the elliptic paraboloid with the same values of $\xi\Lambda_1$ and $\xi\Lambda_2$ in Eq. (20). A dotted straight line is drawn at the level of $\tau/\tau_p=1.0$. In the simulations of diffusion on spheroids, $5.0e-3$ μm, but not the usual value $2.0e-2$ μm, is used as Δr. On the other hand, ξ is 0.1 μm as in the other simulations. Since a function $C(r)$ is calculated all over the surface, the domain of the function varies according to the size of a spheroid.

values all over their surfaces, respectively. However, in the case of a sphere, the effects of the limited area masks the effects of Gaussian curvature as shown in this section. On the other hand, a pseudosphere has surface points at which a function to represent the shape is not differentiable and therefore diffusion is hard to simulate. By comparison with a sphere and a pseudosphere, elliptic and hyperbolic paraboloids, which are used in the present study, are suitable for simulations to examine the effects of positive and negative values of K on diffusion as well as catenoids of Eq. (22) and hyperboloids of Eq. (25) although K is not constant all over the surfaces.

IV. DISCUSSION

To analyze lateral diffusion of membrane molecules, we started from Eq. (1), the diffusion equation in a two-dimensional manifold that has been generally accepted. The solutions of Eq. (3), the equivalent equation in a polar coordinate system, indicate that diffusion proceeds more slowly and faster on surfaces of $K>0$ and $K<0$ than on the plane, respectively. In addition, diffusion is anisotropic at a surface region where the normal curvature is anisotropic and K has nonzero values. The anisotropy is classified into several types. The simulations of diffusion on various surfaces suggest that such effects of Gaussian curvature take place in any type of surfaces. In the following sections, we discuss the meanings of the simulations.

A. ξ as the time of observation

1. Diffusion viewed from a special coordinate system of space and time

In the present simulations, equations to represent various surfaces are written using X, Y, and Z that denote x/ξ, y/ξ, and z/ξ. If values of $\xi\Lambda_1$ and $\xi\Lambda_2$ are given, Eqs. (20), (22), and (24)–(26) are completely determined. Each equation provides an infinite number of surfaces because Λ_1 and Λ_2 have various values according to a value of ξ. One surface determined by one value of ξ corresponds to one diffusion because, on the surface, membrane molecules are initially confined in a circular region of radius ξ. One set of values of $\xi\Lambda_1$ and $\xi\Lambda_2$ thus represents an infinite number of diffusions. For instance, one is a diffusion on a gently curved surface in which ξ has a large value. Another is a diffusion on a sharply curved surface in which ξ has a small value. However, if we view the surfaces from the coordinate system of X, Y, and Z, they are the same surface and the radius of a circular region of C_0 at $t=0$ is always equal to 1.0 because ξ is a unit of the length. Therefore an infinite number of diffusions represented by one set of values of $\xi\Lambda_1$ and $\xi\Lambda_2$ are viewed as the same diffusion taking place on the same surface from the coordinate system of X, Y, and Z. To confirm that the diffusions are certainly the same, the solution of the equation to express diffusion on surfaces is analyzed. Viewing diffusion in such a way is equivalent to replacing r with $\nu=\xi^{-1}r$ in Eq. (3). Moreover, we replace t with $\alpha=\xi^{-2}Dt$. Since a function G is viewed as $H=\xi^{-2}G$ because of Eq. (10), this transformation of coordinates changes Eq. (3) into

$$C_\alpha = C_{\nu\nu} + 0.5H^{-1}H_\nu C_\nu + H^{-1}C_{\theta\theta} - 0.5H^{-2}H_\theta C_\theta. \quad (31)$$

The solution of Eq. (3) depends on a value of D, a function G, the initial conditions determined by a value of ξ and boundary conditions. On the other hand, the solution of Eq. (31) depends on a function H and boundary conditions. In the cases of the surfaces defined by the above-mentioned equations, H is a function of $\xi\Lambda_1$ and $\xi\Lambda_2$ because the function is determined by the shape of surfaces viewed from the coordinate system of X, Y, and Z. Furthermore, since the surfaces infinitely extend in every direction, we can always

use $C(\nu=\pm\infty,\theta,t)=0$ as boundary conditions in solving Eq. (31) analytically. So the solution of Eq. (31) is determined only by $\xi\Lambda_1$ and $\xi\Lambda_2$. In other words, all diffusions represented by one set of values of $\xi\Lambda_1$ and $\xi\Lambda_2$ proceed in the same manner in the space-time system of X, Y, Z, and α. Therefore C at the zero point decreases to $0.5C_0$ during the same time. If the time is represented by $\alpha=M$, we obtain

$$\xi^{-2}D\tau = M. \tag{32}$$

Here M is a function of $\xi\Lambda_1$ and $\xi\Lambda_2$. Since M is constant in the case of the plane,

$$\xi^{-2}D\tau_p = M_0. \tag{33}$$

The simulations of diffusion on the plane indicates that M_0 is approximately 0.44. In the present simulations, D and ξ of diffusion on surfaces have the same values as those of the conventional diffusion on the plane. So the ratio τ/τ_p is equal to M/M_0, which is a function of $\xi\Lambda_1$ and $\xi\Lambda_2$. Indeed, the graphs of τ/τ_p did not change even if a value of D varied (data not shown).

In the case of spheroids defined by Eq. (30), the shape viewed from the coordinate system of X, Y, and Z is determined by values of $\xi\Lambda_1$ and c. Here $\xi\Lambda_1$ is always equal to $\xi\Lambda_2$. The boundary conditions for solving Eq. (31) are $C(\nu=0.5L,\theta,t)=C(\nu=-0.5L,\theta,t)$, where L denotes the perimeter of an elliptical section by the zx plane. Since surfaces viewed as the same shape from the coordinate system of X, Y, and Z have the same value of L, the solution of Eq. (31) is determined by $\xi\Lambda_1$ and c. Therefore Eq. (32) is true with regard to diffusion on spheroids although M is a function of the two variables.

2. Meanings of the functions τ/τ_p and $\langle r^2\rangle/_p\langle r^2\rangle$ of $\xi\Lambda_1$ and $\xi\Lambda_2$

If values of $\xi\Lambda_1$ and $\xi\Lambda_2$ are given in Eq. (20), the set of two values represents an infinite number of diffusions on elliptic paraboloid although they are viewed as the same diffusion from the coordinate system of X, Y, Z, and α. For instance, in the case of $\xi\Lambda_1=\xi\Lambda_2=2.0$, one diffusion takes place on a surface of $\Lambda_1=\Lambda_2=0.4\ \mu\text{m}^{-1}$ and, at the beginning of the diffusion, membrane molecules are confined in a circular region whose radius ξ is 5 μm. Another diffusion takes place on a surface of $\Lambda_1=\Lambda_2=20\ \mu\text{m}^{-1}$ and a value of ξ is 0.1 μm. The rates of the two diffusions deviate from the rate of the normal diffusion on the plane to the same extent because the ratios τ/τ_p and $\langle r^2\rangle/_p\langle r^2\rangle$, which represent the degree of the deviation, are 1.17 and 0.89, respectively, in both cases [Figs. 1(d) and 1(e)]. However, the times during which diffusion is slowed down to such a degree differ for the two diffusions. In other words, the times necessary for observing such a degree of deviation from the normal diffusion in the two cases are different. The observation of diffusion on a surface for a time equal to τ is necessary for determining the value of τ/τ_p. On the other hand, the observation for τ_p is necessary for determining the value of $\langle r^2\rangle/_p\langle r^2\rangle$ because $\langle r^2\rangle$ is calculated at $t=\tau_p$ in the present simulations (see Sec. II). Equation (32) indicates that τ is proportional to ξ^2 if values of $\xi\Lambda_1$ and $\xi\Lambda_2$ are constant. Furthermore, Eq. (33) indicates that τ_p is always proportional to ξ^2. Therefore the time necessary for detecting the stated degree of slowed diffusion is 2500 times longer in the former diffusion of $\xi=5$ μm and $\Lambda_1=\Lambda_2=0.4\ \mu\text{m}^{-1}$ than in the latter one of $\xi=0.1$ μm and $\Lambda_1=\Lambda_2=20\ \mu\text{m}^{-1}$. While this discussion is relevant to the case of positive K, we can similarly discuss the case of negative K using Figs. 3(b) and 3(c). Therefore as the absolute values of Λ_1 and Λ_2 increase, that is, as a surface curves more sharply, diffusion is slowed down or accelerated to a fixed degree for a shorter time because a value of ξ decreases. In other words, while membrane molecules quickly experience the effects of Gaussian curvature on a sharply curved surface, a much longer time is necessary for undergoing the same extent of effects on a gently curved surface. A value of ξ can be thus used as an index of the time during which diffusion is slowed down or accelerated to the degree represented by τ/τ_p and $\langle r^2\rangle/_p\langle r^2\rangle$.

In the above discussion, values of $\xi\Lambda_1$ and $\xi\Lambda_2$ are constant. Next, the case is considered in which values of $\xi\Lambda_1$ and $\xi\Lambda_2$ vary by changing a value of ξ and keeping values of Λ_1 and Λ_2 constant. A straight line passing through the origin is drawn on the $\xi\Lambda_1$-$\xi\Lambda_2$ plane. The increase in a value of ξ at constant values of Λ_1 and Λ_2 is equivalent to going along the straight line away from the origin. Even if values of $\xi\Lambda_1$ and $\xi\Lambda_2$ change in such a way, ξ can be regarded as an index of the time during which diffusion is slowed down or accelerated to the degree represented by τ/τ_p and $\langle r^2\rangle/_p\langle r^2\rangle$ for the following reasons. While τ is proportional to $\xi^2 M$ [see Eq. (32)], M does not change dramatically in comparison with ξ^2 because τ/τ_p that is equal to M/M_0 is never proportional to ξ^2 as shown in Figs. 1(d) and 3(b). So τ is roughly proportional to ξ^2. On the other hand, τ_p is proportional to ξ^2 [see Eq. (33)]. Figures 1(d) and 1(e) indicate that τ/τ_p increases and $\langle r^2\rangle/_p\langle r^2\rangle$ decreases as a value of ξ increases along the straight line drawn on the $\xi\Lambda_1$-$\xi\Lambda_2$ plane. In contrast, Figs. 3(b) and 3(c) indicate that τ/τ_p decreases and $\langle r^2\rangle/_p\langle r^2\rangle$ increases as ξ increases along the straight line. Therefore the diffusion rate on surfaces that are the same due to constant values of Λ_1 and Λ_2 deviates from the rate of the ordinary diffusion on the plane more greatly as the time of observation gets longer. In other words, the degrees of slowed and accelerated diffusions in the cases of $K>0$ and $K<0$ become greater as diffusion on the same surface is observed for a longer time. Here "the same surface" is mentioned in the view from the usual coordinate system of x, y, and z. It is viewed as various surfaces from the coordinate system of X, Y, and Z because $\xi\Lambda_1$ and $\xi\Lambda_2$ have different sets of values when a value of ξ is changed keeping values of Λ_1 and Λ_2 constant.

Next, we calculate the apparent diffusion coefficient D_{app} by defining it to be $\xi^2\tau^{-1}M_0$. If diffusions represented by one point on the $\xi\Lambda_1$-$\xi\Lambda_2$ plane have the same value of D, they have the same value of D_{app} because $\xi^2\tau^{-1}$ is constant at the point as show in Eq. (32). In contrast, two diffusions represented by different points have different values of D_{app} even if they have the same value of D. Equation (33) provides the formula $D_{app}/D=(\tau/\tau_p)^{-1}$, which means that the ratio of D_{app} to D is the reciprocal of τ/τ_p. Therefore the graphs of τ/τ_p such as Figs. 1(d) and 3(b) indicate that the ratio

D_{app}/D decreases down from 1.0 in the case of $K>0$ and increases up from 1.0 in the case of $K<0$ as a value of ξ increases keeping values of Λ_1 and Λ_2 constant, which is equivalent to going along the straight line away from the origin on the $\xi\Lambda_1$-$\xi\Lambda_2$ plane as mentioned above. In other words, D_{app} deviates from D more greatly as the time of observation gets longer even if diffusions take place on the same surface. For instance, two diffusions on elliptic paraboloid represented by $\xi=0.1$ μm and $\Lambda_1=\Lambda_2=20$ μm^{-1} and by $\xi=0.05$ μm and $\Lambda_1=\Lambda_2=20$ μm^{-1} are considered. While the two diffusions take place on the same surface, they are represented by different points on the $\xi\Lambda_1$-$\xi\Lambda_2$ plane because of different sets of values of $\xi\Lambda_1$ and $\xi\Lambda_2$. Since τ/τ_p is 1.17 in the diffusion of $\xi=0.1$ μm and 1.09 in the diffusion of $\xi=0.05$ μm [Fig. 1(d)], D_{app} is 7% smaller in the former diffusion than in the latter one. These analyses suggest that the time of observation affects the diffusion coefficient calculated from the experimental data if the calculation is based on a formula regarding the normal diffusion on the plane like Eq. (33). The diffusion coefficient in inhomogeneous media is generally thought to depend on the observation time or the diffusion length. Recently, the spatiotemporal dependence of such anomalous diffusion was directly shown through FCS using an instrument with which the confocal volume of a microscope can be continuously changed [15]. The dependence of D_{app} on the observation time in diffusion on surfaces is theoretically predicted here. In addition, diffusion on surfaces seems to be anomalous because $\langle r^2\rangle$ deviates from ${}_p\langle r^2\rangle$ as shown in Fig. 1(e). Although $\langle r^2\rangle$ in the present simulations does not correspond to the mean-square displacement in a strict sense (see Sec. II), it is shown later that, at least, diffusion for a short time is certainly anomalous [see Eq. (39)]. Therefore diffusion on surfaces is similar to anomalous diffusion in an inhomogeneous system.

3. Diffusion-limited reactions

If a value of D is given, ξ can be regarded as a function of τ_p on the basis of Eq. (33). The function is denoted by $\xi(\tau_p)$. If something related to lateral diffusion takes place on a surface of Λ_1 and Λ_2 for a time equal to τ_p, Gaussian curvature may have the effects represented by $\langle r^2\rangle/{}_p\langle r^2\rangle$ at the values of $\xi(\tau_p)\Lambda_1$ and $\xi(\tau_p)\Lambda_2$ on it. Diffusion-limited phenomena are likely to be affected more greatly on a sharply curved surface than on a gently curved surface if the phenomena occur for the same time. To make the discussion more concrete, a chemical reaction among membrane molecules, which is limited by diffusion, is considered. If one membrane molecule as enzyme collides with substrate molecules 100 times per second in the plane membrane, the mean interval between two collisions is 0.01 s. In the case of $D=3.162e-9$ cm^2 s^{-1}, $\xi(\tau_p)$ is 0.08 μm at $\tau_p=0.01$ s, which is calculated using $M_0=0.44$. On a surface of $\Lambda_1=\Lambda_2=20$ μm^{-1}, the observation for 0.01 s gives the deviation from the ordinary diffusion represented by $\langle r^2\rangle/{}_p\langle r^2\rangle=0.91$ because of $\xi\Lambda_1=\xi\Lambda_2=1.6$ in Fig. 1(e). On a surface of $\Lambda_1=\Lambda_2=0.4$ μm^{-1}, which curves much more gently, the observation for the same time gives the deviation represented by $\langle r^2\rangle/{}_p\langle r^2\rangle=0.9997$ because of $\xi\Lambda_1=\xi\Lambda_2=0.032$. Therefore the mean interval between two collisions may get longer than 0.01 s on the former surface and is likely to remain unchanged on the latter one. It means that the reaction velocity decreases on surfaces of large positive values of K. Since the case of $K<0$ can be similarly discussed using Fig. 3(c), the reaction velocity may increase on surfaces where the absolute values of negative K are large. If Gaussian curvature affects the reaction velocity, the shape of membranes directly influences the reactions taking place in them.

Some surfaces of positive values of K have the finite area. The ratio τ/τ_p is much larger than 1.0 in diffusion on such closed surfaces if the whole area is small [Fig. 6(b)]. Diffusion-limited reactions may proceed slowly in small closed membranes such as vesicles due to not only positive K but also the limited area. However, it remains to be examined whether the limited area really affects the reaction velocity by reducing the diffusion rate.

B. Possible geometry that causes the effects of Gaussian curvature

1. Way to introduce the effects of Gaussian curvature into Monte Carlo simulations

Biological membranes are more complicated than surfaces treated in the present simulations. It is not easy to simulate diffusion on real membranes by directly solving Eq. (1) in a two-dimensional coordinate system such as a geodesic polar coordinate system. This is one of the reasons why Monte Carlo methods are frequently used for simulations of diffusion on curved biomembranes. According to the methods, a particle moves from one surface point to another point for a time unit. Since the path from the initial point to the next point is not considered, the movement may be called a "jump." The time unit is denoted by ε. Since ε is very short in most cases, one jump is usually performed on the tangent plane touching a surface at the initial point [3,9]. The particle is projected back to the surface after the jump. However, the effects of Gaussian curvature, i.e., slowdown or acceleration and anisotropy of diffusion, do not seem to be sufficiently considered when simulations are carried out by repeating such a jump. If K has a small positive value, the jump on the tangent plane may provide pretty good simulations. On the other hand, if K has a large positive value or a negative value, simulations are likely to deviate from the analytical solutions of Eq. (1). One way to efficiently introduce the effects of Gaussian curvature into simulations is to perform the jump on a surface. By taking the initial point as the zero point of $r=0$, a geodesic polar coordinate system can be locally defined on a surface represented by $\nabla\phi(x,y,z)=0$. We can numerically calculate the function $G(r,\theta)$ by regarding x and y in $\nabla\phi=0$ as two-dimensional parameters of the surface, i.e., u and v (see Sec. II). In the case of diffusion on the plane, the expression $(1/4\pi D\varepsilon)\exp(-r^2/4D\varepsilon)(r^2)^{0.5}\,dr\,d\theta$ represents the probability that, after a jump from the zero point, a particle exists at a quadrilateral region consisting of four points of (r,θ), $(r+dr,\theta)$, $(r,\theta+d\theta)$, and $(r+dr,\theta+d\theta)$. It is assumed that the expression $[1/L(\varepsilon)]\exp(-r^2/4D\varepsilon)G^{0.5}\,dr\,d\theta$ represents the probability in the case of diffusion on surfaces. Here the term of

$G^{0.5}\,dr\,d\theta$ represents the area of the quadrilateral region on surfaces. A geodesic circle with its center located at the initial point is considered. If the radius κ of the geodesic circle is two or three times larger than $(4D\varepsilon)^{0.5}$, most particles exist within the circle after the jump. Therefore we obtain

$$L(\varepsilon) = \int_0^{2\pi} \int_0^{\kappa} \exp(-r^2/4D\varepsilon) G^{0.5}\, dr\, d\theta. \tag{34}$$

To make the calculation easier to understand, r and θ are defined on the intervals $0 \leqslant r \leqslant \kappa$ and $0 \leqslant \theta < 2\pi$, but not the intervals $-\kappa \leqslant r \leqslant +\kappa$ and $0 \leqslant \theta < \pi$. Equation (34) provides the same function of $L(\varepsilon)$, whichever of the two types of intervals is used as the domains of the integrand. The right-hand side of Eq. (34) can be analytically calculated in the following way. If a value of r is so small, the circumference of a geodesic circle of radius r is equal to $2\pi r - (\pi/3)Kr^3$. Here K represents Gaussian curvature at the center of the geodesic circle. Since the value of κ is small and r is smaller than κ,

$$\int_0^{2\pi} G^{0.5}\, d\theta = 2\pi r - (\pi/3)Kr^3 \quad (0 \leqslant r \leqslant \kappa). \tag{35}$$

The double integral in the right-hand side of Eq. (34) can be calculated using this relation. Since most particles exist within the geodesic circle of radius κ after the jump, $\exp(-\kappa^2/4D\varepsilon)$ is close to zero. Therefore we obtain

$$L(\varepsilon) = 4\pi D\varepsilon - (8\pi/3)KD^2\varepsilon^2. \tag{36}$$

Since $L(\varepsilon)$ must be positive, a value of ε has to be selected in a manner such that the relation $\varepsilon < 1.5(KD)^{-1}$ holds. One set of values of r and θ, which corresponds to one jump, can be drawn from the intervals $0 \leqslant r \leqslant \kappa$ and $0 \leqslant \theta < 2\pi$ on the basis of $[1/L(\varepsilon)]\exp(-r^2/4D\varepsilon)G^{0.5}\,dr\,d\theta$, the expression representing the probability. We can perform the simulations more easily by using Eq. (36) than by numerically calculating the right-hand side of Eq. (34).

2. Effects of Gaussian curvature on a short-time diffusion

To examine whether the above-mentioned method produces the effects of Gaussian curvature in the simulations, the probability density function (PDF) and the mean-square displacement are calculated. Equation (36) gives

$$P(r,\theta,t=\varepsilon) = [1/\{4\pi D\varepsilon - (8\pi/3)KD^2\varepsilon^2\}]\exp(-r^2/4D\varepsilon), \tag{37}$$

where $P(r,\theta,t=\varepsilon)$ denotes the probability density function after one jump. This formula indicates that, at all points within the geodesic circle of radius κ, the PDF has larger and smaller values in the cases of $K>0$ and $K<0$ than in the case of the plane, respectively. Since the molecular concentration C is proportional to the PDF, diffusion is slower and faster on surfaces of $K>0$ and $K<0$ than on the plane, respectively. The mean-square displacement $\langle r^2 \rangle$ is calculated as

$$\langle r^2 \rangle = \int_0^{2\pi} \int_0^{\kappa} r^2 P(r,\theta,t=\varepsilon) G^{0.5}\, dr\, d\theta. \tag{38}$$

By substituting Eq. (37) for this formula, the mean-square displacement can be expressed as

$$\langle r^2 \rangle = 4D\varepsilon - 8KD^2\varepsilon^2(3 - 2KD\varepsilon)^{-1}. \tag{39}$$

Equation (35) and $\exp(-\kappa^2/4D\varepsilon)=0$ are used for calculating this relation. The term $3-2KD\varepsilon$ is positive because of $\varepsilon < 1.5(KD)^{-1}$. Therefore the mean-square displacement is smaller and lager in the cases of $K>0$ and $K<0$ than $4D\varepsilon$, the ordinary value of $\langle r^2 \rangle$ in the case of the plane, respectively. These results indicate that nonzero values of Gaussian curvature affect the diffusion rate even if diffusion is observed for a very short time. On the other hand, anisotropic diffusion does not take place for such a short time because $P(r,\theta,t=\varepsilon)$ is a function of only r in Eq. (37). However, the presence of the function $G(r,\theta)$ in $P(r,\theta,t=\varepsilon)G^{0.5}\,dr\,d\theta$, the expression representing the probability, has anisotropic effects on one jump of a particle. Anisotropic diffusion may result from repeating such a jump.

C. Effects of Gaussian curvature are fundamental in considering lateral diffusion of membrane molecules

The sorts and ratio of lipids and proteins that constitute the lipid bilayer may vary according to the membrane curvature in biological membranes. If so, there is a possibility that not only Gaussian curvature but also mean curvature influences lateral diffusion of mobile components through the heterogeneity of membrane structures. Furthermore, a recent theoretical study indicates that membrane curvature affects the fluidity of a membrane through changes in its thickness and consequently the diffusion rate of membrane molecules varies [16]. In this study, the effects of mean curvature were mainly analyzed and the predicted diffusion coefficients were consistent with experimental data [17]. Since Gaussian curvature is likely to change the membrane thickness as well as mean curvature, both of the two curvatures may affect the diffusion rate through such a mechanism. While membrane curvature has effects on lateral diffusion in various ways, the effects of Gaussian curvature predicted in the present study may be one of important factors that influence the diffusion process of membrane molecules. It is because the effects are inevitable for all laterally mobile molecules as long as they move along surfaces where Gaussian curvature has nonzero values. Moreover, the predicted effects are not quantitatively negligible in many cases. For instance, human erythrocytes are biconcave disk-shaped cells with diameter of approximately 8 μm and thickness of approximately 2 μm at the outer rim. We can say that, in a lateral region of the cell, Λ_1 and Λ_2 are approximately 0.25 and 1.0 $\mu\mathrm{m}^{-1}$, respectively. If an approximation of the shape of the lateral region is made using elliptic paraboloid and the diffusion coefficient of membrane molecules is $3.162e{-}9\ \mathrm{cm}^2\,\mathrm{s}^{-1}$, $\xi(\tau_p)\Lambda_1$ and $\xi(\tau_p)\Lambda_2$ are equal to 0.5 and 2.0 at $\tau_p=6$ s, respectively. The value of τ_p is calculated using Eq. (33) in which M_0 is 0.44. Therefore it is predicted that $\langle r^2 \rangle$ is 6% smaller than ${}_p\langle r^2 \rangle$ when molecules diffuse for 6 s [Fig. 1(e)]. In addition to

slowed diffusion, the $+K1$ type of anisotropic diffusion is likely to take place [Fig. 2(g)]. Diffusion is the slowest in the direction along the diameter of the disklike cell and the fastest in the direction perpendicular to it [Fig. 2(f)]. Anisotropy of diffusion on a surface of $\xi\Lambda_1=2.0$ and $\xi\Lambda_2=0.5$, which is identical to anisotropy of diffusion on the surface of $\xi\Lambda_1=0.5$ and $\xi\Lambda_2=2.0$ simulated here, is shown as graph lines marked with small circles in Figs. 2(c) and 2(d). Therefore, in diffusion for 6 s, $\langle r^2\rangle^*$ is 10% smaller in the direction along the cell diameter than in the direction perpendicular to it [Fig. 2(d)]. For another instance, if the diameter of a microvillus is 0.1 μm and the shape of a region around the tip is close to a half sphere, values of Λ_1 and Λ_2 at the tip are 20 μm^{-1}. If an approximation of the shape is made using elliptic paraboloid and D is $3.162e-9$ $cm^2\ s^{-1}$, $\xi(\tau_p)\Lambda_1$ and $\xi(\tau_p)\Lambda_2$ are equal to 2.0 at $\tau_p=14$ ms [Fig. 1(e)]. So it is predicted that $\langle r^2\rangle$ is 11% smaller than ${}_p\langle r^2\rangle$ when molecules diffuse for 14 ms. In these cases, the deviation from the rate of the ordinary diffusion on the plane and the degree of anisotropy seem to be too large to ignore. However, it remains to be examined whether Gaussian curvature causes significant biological phenomena through the change in the diffusion rate and anisotropy of diffusion.

Real membranes thermally fluctuate so that membrane curvature fluctuates. It is theoretically predicted that curvature fluctuations decrease the diffusion rate by increasing the average membrane thickness and the geometric path length [16,18] although the possibility is pointed out that the fluctuations sometimes increase the diffusion rate [18]. When Gaussian curvature fluctuates due to membrane undulations, how does the diffusion rate change? If K continues to have either positive or negative values throughout the fluctuations, diffusion may be made slower or faster, respectively. In the case of positive K, the fluctuating Gaussian curvature reduces the diffusion rate together with the enlarged membrane thickness and the growing geometric path length. In the case of negative K, the fluctuating curvature increases the diffusion rate against the effects of the membrane thickness and the geometric path length. If K takes both positive and negative values during the fluctuations, the total effects of Gaussian curvature depend on how membranes undulate. The mathematical method of dealing with diffusion on surfaces whose shape varies with time is necessary for quantitatively analyzing the effects of fluctuating Gaussian curvature on the diffusion process.

Several lines of evidence have demonstrated that the cell membrane is compartmentalized with regard to lateral diffusion of membrane proteins and lipids [19,20]. Membrane molecules are temporarily confined in a compartment and occasionally hop to an adjacent compartment. So they undergo both diffusion within compartments and hop diffusion over many compartments. While the former microscopic diffusion takes place for a short time, the latter macroscopic one is detected through the observation for a longer time. Effects of Gaussian curvature have to be considered in both microscopic and macroscopic diffusions. For instance, phospholipids are confined in a compartment with diameter of 230 nm and the diffusion coefficient is 5.4 $\mu m^2\ s^{-1}$ when measured in a 100-μs time window [20]. Since 100 μs, the period for which diffusion is observed, is very short, Eq. (39) can be used for analyzing this case. While 100 μs can be regarded as a value of ε, the mean-square displacement is equal to 5.4 $\mu m^2\ s^{-1}$ multiplied by 4ε. When values of ε and $\langle r^2\rangle$ are thus given in Eq. (39), K is a function of D. In the case of $K>0$, according to the function, the square root of K is approximately 15 μm^{-1} if the real value of D is 10% larger than 5.4 $\mu m^2\ s^{-1}$, the measured value of D. In other words, the real D has a value greater than 110% of the measured D if the membrane of a compartment curves more sharply than the surface of $(\Lambda_1\Lambda_2)^{0.5}=15$ μm^{-1}. In the case of $K<0$, the real D has a value less than 90% of the measured D if the membrane of a compartment curves more sharply than the surface of $(-\Lambda_1\Lambda_2)^{0.5}=18$ μm^{-1}. Although such a surface is pretty steep, the vigorous deformation of local membranes may be caused by various factors such as reorganization of membrane skeletons and thermal undulations of membranes. Indeed, Brown pointed out the theoretical possibility that thermal membrane undulations are active enough to cause occasional hopping to an adjacent compartment [21]. Considering that compartments are so small, the possibility cannot be ruled out that Gaussian curvature affects the rate of diffusion within a compartment. On the other hand, the square root of the mean-square displacement is approximately 50 nm and the diameter of a compartment is 230 nm. Therefore the diffusion observed for 100 μs does not seem to be influenced by the limited area as shown in Fig. 6(b). In other words, it is unlikely that the real value of D is much larger than 5.4 $\mu m^2\ s^{-1}$ because of the effects of the limited area. It is, however, difficult to estimate the degree of the effects of the limited area because phospholipids are not completely confined in a compartment. With regard to hop diffusion over compartments, the diffusion coefficient of phospholipids is 0.42 $\mu m^2\ s^{-1}$ when measured in a 3-s time window [20]. The case is considered in which the real value of D is larger than the measured value of D due to positive K. The real value of D is equivalent to the diffusion coefficient obtained from data of the diffusion on the plane membrane. So $\langle r^2\rangle/{}_p\langle r^2\rangle$ can be used as an approximation of the ratio of the measured D to the real D although $\langle r^2\rangle$ in the present study is not identical to the mean-square displacement in a strict sense (see Sec. II). If an approximation of the shape of the membrane is made using parabolic surfaces, Fig. 1(e) indicates that $\xi\Lambda_1$ and $\xi\Lambda_2$ are equal to 1.55 at $\langle r^2\rangle/{}_p\langle r^2\rangle=1/1.1$, which means that the real D is 10% larger than the measured D. We can calculate ξ by entering 3 s and 0.462 $\mu m^2\ s^{-1}$, the real value of D given here, into τ_p and D in Eq. (33). Since ξ is 1.77 μm, diffusion takes place on the surface of $\Lambda_1=\Lambda_2=0.87$ μm^{-1} in this case. So it is predicted that, regarding the diffusion observed for 3 s, the real D has a value greater than 110% of the measured D if the membrane curves more sharply than the surface of $\Lambda_1=\Lambda_2=0.87$ μm^{-1}. Since such surfaces are never steep, the effects of Gaussian curvature on the diffusion coefficient obtained through the observation for 3 s may not be negligible even when diffusion takes place on a gently curved surface.

To estimate the degree to which diffusion is affected by Gaussian curvature is thus necessary for analyzing the diffusion process on curved membranes. If the effects are too

large to neglect, Gaussian curvature may play an important role in diffusive phenomena although the real diffusion process is affected by various factors other than Gaussian curvature. It seems that Gaussian curvature has large absolute values and the normal curvature is anisotropic frequently in many regions of real membranes in part because their local and global shapes continuously change. So there is a strong possibility that lateral diffusion of membrane molecules proceeds at different rates according to place and is usually anisotropic.

[1] R. N. Ghosh and W. W. Web, Biophys. J. **66**, 1301 (1994).
[2] P. R. Smith, I. E. G. Morrison, K. M. Wilson, N. Fernández, and R. J. Cherry, Biophys. J. **76**, 3331 (1999).
[3] M. Weiss, H. Hashimoto, and T. Nilsson, Biophys. J. **84**, 4043 (2003).
[4] M. J. Saxton, Biophys. J. **81**, 2226 (2001).
[5] B. A. Smith, W. R. Clark, and H. M. McConnell, Proc. Natl. Acad. Sci. U.S.A. **76**, 5641 (1979).
[6] J. B. de Monvel, W. E. Brownell, and M. Ulfendahl, Biophys. J. **91**, 364 (2006).
[7] B. M. Aizenbud and N. D. Gershon, Biophys. J. **38**, 287 (1982).
[8] B. M. Aizenbud and N. D. Gershon, Biophys. J. **48**, 543 (1985).
[9] R. Holyst, D. Plewczyński, A. Aksimentiev, and K. Burdzy, Phys. Rev. E **60**, 302 (1999).
[10] I. F. Sbalzarini, A. Hayer, A. Helenius, and P. Koumoutsakos, Biophys. J. **90**, 878 (2006).
[11] T. Yoshigaki, Bull. Math. Biol. **64**, 643 (2002).
[12] T. Yoshigaki, J. Theor. Biol. **221**, 229 (2003).
[13] M. Christensen, J. Comput. Phys. **201**, 421 (2004).
[14] S. Kobayashi, *Differential Geometry of Curves and Surfaces*, 26th ed. (Shokabo, Tokyo, 1998).
[15] A. Masuda, K. Ushida, and T. Okamoto, Phys. Rev. E **72**, 060101 (2005).
[16] N. S. Gov, Phys. Rev. E **73**, 041918 (2006).
[17] Y. Gambin, G. Massiera, L. Ramos, C. Ligoure, and W. Urbach, Phys. Rev. Lett. **94**, 110602 (2005).
[18] E. Reister and U. Seifert, Europhys. Lett. **71**, 859 (2005).
[19] A. Kusumi, Y. Sako, and M. Yamamoto, Biophys. J. **65**, 2021 (1993).
[20] T. Fujiwara, K. Ritchie, H. Murakoshi, K. Jacobson, and A. Kusumi, J. Cell Biol. **157**, 1071 (2002).
[21] F. L. H. Brown, Biophys. J. **84**, 842 (2003).